Performance Analysis of Locally Most Powerful Invariant Test for Sphericity of Gaussian Vectors in Coherent MIMO Radar

Yu-Hang Xiao, *Student Member, IEEE*, Lei Huang, *Senior Member, IEEE*, Jian-Kang Zhang, *Senior Member, IEEE*, Junhao Xie, *Senior Member, IEEE*, and Hing Cheung So, *Fellow, IEEE*

***Abstract*—Locally most powerful invariant test (LMPIT) for sphericity of Gaussian vectors has been derived by Ramírez *et al.* Nevertheless, the decision threshold of the LMPIT is not accurate and its detection performance has not yet been addressed. In this paper, the LMPIT is performed for target detection in multiple-input multiple-output (MIMO) radar, and its theoretical decision threshold as well as detection probability are accurately determined. Utilizing asymptotic expansion approach, we calculate the asymptotic null distribution as a function of central chi-square distributions, resulting in precise closed-form formula for thresholding. On the other hand, the nonnull distribution is approximated by weighted sum of noncentral chi-square distributions and Gamma distribution for close and far hypotheses, respectively. This enables us to derive a closed-form formula to precisely evaluate the detection power of the LMPIT. Numerical results demonstrate that our theoretical computations are very accurate in determining the decision threshold and predicting the behaviors of the LMPIT. Moreover, the superiority of the LMPIT for MIMO radar target detection over state-of-the-art methods is demonstrated for spatially colored but temporarily white noise.**

***Index Terms*—Sphericity test, locally most powerful invariant test, asymptotic series expansion, chi-square approximation, threshold calculation, coherent MIMO radar detection.**

I. Introduction

THE problem of testing for sphericity is to infer whether a set of random variables is independent and identically distributed (i.i.d.) or not, or equivalently, to test the null hypothesis that the covariance matrix is an identity matrix multiplied by an unknown scalar. Such an issue is widely seen in a number of application areas such as signal detection in sonar and radar [2], [3], source number estimation [4], image processing [5] and spectrum sensing [6]–[8]. In the real-valued Gaussian case, Mauchly [9] first derived the generalized likelihood ratio test (GLRT) for this hypothesis testing problem, which, however, is suboptimal as signal-to-noise ratio (SNR) becomes small. To tackle this drawback, John [10] derived the locally most powerful invariant test (LMPIT) for sphericity. Later on, Nagao [11] independently reached the same test statistic as John's test by exploiting the asymptotic variance of the GLRT. More recently, Ramírez *et al.* [1] generalized this problem to the vector case, where the covariance matrix under the null hypothesis is the Kronecker product of the identity matrix and an unknown matrix, and derived the LMPIT for this detection problem under both real- and complex-valued scenarios.

The need of sphericity test for vectors arises from applications such as coherent multiple-input multiple-output (MIMO) radar detection. Unlike traditional radar, the coherent MIMO radar can transmit linearly independent waveforms, which are known at the receiver, to achieve coherent processing gain. One challenging issue in MIMO radar target detection is that the noise covariance structure is usually not available and may be unspecified. Thus, it is not possible to distinguish signals from the unknown background noise by their covariance matrices. To address this problem, an additional reference channel could be equipped to collect target-free secondary data, which are used to estimate the noise covariance matrix at the receiver, thereby improving the robustness of the detector against colored noise [12]–[16]. However, the overhead increases system complexity and requires the noise in the reference and surveillance channels to share the same statistical properties; otherwise, the detection performance might be degraded. As a matter of fact, in coherent MIMO radar, the receiver can utilize linear independence between the waveforms and perform pulse compression and vectorization to dissimilate the covariance matrices under the target presence and absence cases. Since the waveforms are linearly independent, the pulse compression can retain the independence between the column vectors of the noise data matrix while correlate those of the signal part. Thus, after vectorization, the noise covariance matrix becomes block-spherical. Such a noise covariance matrix structure guarantees the identifiability

Manuscript received October 21, 2017; revised December 20, 2017; accepted January 17, 2018. Date of publication February 5, 2018; date of current version July 16, 2018. This work was supported in part by the National Natural Science Foundation of China under Grants U1713217 and U1501253, in part by the Natural Science foundation of Guangdong Province under Grant 2015A030311030, and in part by the Foundation of Shenzhen City under Grant ZDSYS201507081625213. The work of Y.-H. Xiao was supported by the China Scholarship Council. The review of this paper was coordinated by Dr. C. Yuen. *(Corresponding author: Lei. Huang.)*

Y.-H. Xiao and J. Xie are with the Department of Electronic Engineering, Harbin Institute of Technology, Harbin 150001, China (e-mail: yuhangxiao@outlook.com; xj@hit.edu.cn).

L. Huang is with the College of Information Engineering, Shenzhen University, Shenzhen 518060, China (e-mail: dr.lei.huang@ieee.org).

J.-K. Zhang is with the Department of Electrical and Computer Engineering, McMaster University, Hamilton, ON L8S 4L8, Canada (e-mail: jkzhang@mail.ece.mcmaster.ca).

H. C. So is with the Department of Electronic Engineering, City University of Hong Kong, Hong Kong (e-mail: hcso@ee.cityu.edu.hk).

Color versions of one or more of the figures in this paper are available online at http://ieeexplore.ieee.org.

Digital Object Identifier 10.1109/TVT.2018.2801802

of target echoes. However, the state-of-the-art approaches have not yet utilized this property. The reason is that they have usually used the Swerling-I model, in which the coherent process interval (CPI) is long and the reflection coefficient is modeled as a constant. Therefore, the received data are compressed into only one vector, and second-order statistics are not of interest. When the CPI is short, the reflection coefficient should be modeled as a random variable (Swerling-II model [18]), leading to a sequence of i.i.d. output data vectors. Under these circumstances, it is desirable to exploit the specific structure of the noise covariance matrix. In particular, the source detection problem can be cast as detecting whether the covariance matrix of the vectorized data is block spherical or not [1]. In practical implementations, there are two well-known criteria to produce CFAR detectors, i.e., the generalized likelihood ratio (GLR) and locally most powerful invariant (LMPI). Usually, the implementation of the GLR criterion is straightforward while that of the LMPI requires one to firstly seek the maximal invariant statistic, then determine the ratio of its probability densities under the binary hypotheses, which is quite non-trivial. However, the LMPI criterion always leads to "locally optimal" detectors that perform particularly well in the low SNR regime. Since the MIMO radar usually needs to detect very weak target echos, the LMPIT, derived by the LMPI criterion in [1], is a good candidate for this task.

As a matter of fact, the distributions of the LMPIT have not yet been analyzed accurately in the literature, which thereby motivates us to fill this gap. In other words, the aim of this paper is to derive accurate distributions of LMPIT under null and non-null hypotheses, which enables us to set the decision threshold and assess its detection performance precisely. It should be noted that [1] gives an approximation to the null distribution of the LMPIT in the vector case by resorting to the Wilks' theorem [20]. However, this result contains only the dominant term and is not able to yield accurate null distribution, particularly when the sample size becomes small, thus resulting in a relatively large error in the decision threshold. It is worth pointing out that in the real-valued scalar case, Nagao [11] derived asymptotic expansion of the null distribution up to order $\mathbf{o}(n^{-2})$, with n being the sample size. The asymptotic series expansion provides the higher-order terms which are omitted in the limiting distribution, thereby being able to further improve the approximation accuracy. Note that the authors of [8] found that this null distribution is not as accurate as predicted by the remnant's order. Indeed, the inaccuracy is due to calculation errors in [11] rather than the invalidity of the asymptotic expansion method. This is verified by our calculations in this paper, which can be taken as a generalization of the result in [11]. Furthermore, the asymptotic expansion determines the null distribution as a weighted sum of Chi-square distributions, ending up with a computationally simple and invertible function. As a result, we are able to determine the closed-form threshold expression for decision making, significantly reducing the computational cost. On the other hand, we will derive the accurate non-null distribution of the LMPIT.

It should be pointed out that under the non-null hypothesis, the asymptotic expansions of the non-null distributions for high and low SNR regions should be calculated separately, since the covariance matrices possess different asymptotic structures under these two conditions [21], [22]. Therefore, the non-null distribution are approximated separately for the low and SNR cases. In summary, the main contributions of this work include:

1) Under the null hypothesis, we derive the distribution of the LMPIT as a weighted sum of Chi-square distributions by inverting the asymptotic expansion of the characteristic function. The accuracy of the derived distribution is up to order $\mathbf{o}(n^{-2})$.
2) By inverting the null hypothesis, we obtain a closed-form threshold formula for the LMPIT, which avoids numerically inverting the null distribution. As a result, the complexity involved in decision threshold computation is very low.
3) Under the non-null hypothesis, the distribution of the LMPIT is produced in terms of non-central Chi-square distribution with remnant's order $\mathbf{o}(n^{-\frac{3}{2}})$ for the low SNR case. For the high SNR case, we employ the asymptotic expansion method to precisely determine the mean and variance of the LMPIT, resulting in an accurate Gamma approximation to its non-null distribution. This in turn allows us to accurately predict the detection behavior of the LMPIT approach.

The remainder of this paper is structured as follows. Section II presents the hypothesis testing model and LMPIT approach. Section III derives the asymptotic null distribution of the LMPIT along with closed-form expression for threshold calculation. The distribution under the alternative hypotheses is presented in Section IV. Section V provides simulation results to confirm the theoretical calculations. Finally, conclusions are drawn in Section VI.

Throughout this paper, we use boldface uppercase letters for matrices, boldface lowercase letters for column vectors, and normal font letters for scalar quantities. The $\mathbb{E}[a]$ denotes the expectation of a and $\mathbb{V}(a)$ means the variance of a. The $\mathbf{A} \in \mathbb{R}^{p\times n}(\mathbb{C}^{p\times n})$ means that $\mathbf{A}$ is a $p \times n$ real (complex) matrix and $\mathbf{A}_{ij}$ $(\mathbf{A}_{i,j})$ stands for the (i,j) block (element) of $\mathbf{A}$. The $\mathbf{0}_{p\times n}$ denotes the $p \times n$ zero matrix. The $|\mathbf{A}|$ and $||\mathbf{A}||_F$ are the determinant and Frobenius norm of $\mathbf{A}$, respectively. The $\text{tr}(\mathbf{A})$ means the trace of $\mathbf{A}$ and $\text{Tr}(\mathbf{A})$ signifies the summation of all diagonal blocks of $\mathbf{A}$. The $\text{etr}(\mathbf{A})$ stands for $e^{\text{tr}(\mathbf{A})}$. Superscripts $(\cdot)^T$ and $(\cdot)^H$ represent transpose and Hermitian transpose operations. The $(\cdot)^R$ and $(\cdot)^I$ denote the real and imaginary parts, respectively. The $\mathbf{S} \sim \mathcal{CW}_p(n, \mathbf{\Sigma})$ means that $\mathbf{S}$ follows a complex Wishart distribution with n degrees of freedom (DOFs) and associated covariance matrix $\mathbf{\Sigma} \in \mathbb{C}^{p\times p}$ and $\sim$ signifies "distributed as". The $\mathbf{A}^{\frac{1}{2}}$ $(\mathbf{A}^{-\frac{1}{2}})$ is the Hermitian square root of the Hermitian matrix $\mathbf{A}$ $(\mathbf{A}^{-1})$. $\mathbf{A} \otimes \mathbf{B}$ denotes the Kronecker product of $\mathbf{A}$ and $\mathbf{B}$. The $\mathbf{o}(n^i)$ means a scalar whose magnitude is comparable to n^i and $\mathcal{O}(n^i)$ stands for a matrix whose elements are of order n^i. Finally, the exponent of any Hermitian matrix is defined as

$$e^{\mathbf{A}} = \mathbf{I} + \mathbf{A} + \frac{\mathbf{A}^2}{2!} + \frac{\mathbf{A}^3}{3!} + \cdots + \frac{\mathbf{A}^n}{n!} + \cdots, \tag{1}$$

where the power $\mathbf{A}^k$ of a matrix $\mathbf{A}$ for a positive integer k is defined as the matrix product of k copies of $\mathbf{A}$,

$$\mathbf{A}^k = \underbrace{\mathbf{A}\cdots\mathbf{A}}_{k}. \tag{2}$$

II. Problem Formulation

Consider a coherent MIMO radar system where there are q co-located transmit antennas and m co-located receive antennas. The transmitters simultaneously emit q mutually orthogonal waveforms $\mathbf{U} \in \mathbb{C}^{q\times k}$ such that $\mathbf{U}\mathbf{U}^H = \mathbf{I}_q$. The transmitted signals are reflected by a far-field point source located at (θ, φ), with θ and φ being the angles of the target with respect to transmit and receive arrays, respectively, which is stationary during the observation time. The reflection coefficient of the source, denoted as β, is modeled by a zero-mean complex Gaussian variable, and is fixed for each pulse duration but changes independently from pulse to pulse, i.e., it conforms to the Swerling-II model [18]. The receiver collects the reflected signal snapshot by snapshot, and each snapshot corresponds to a pulse duration (k code symbols). Thus, the received data arrived at the receiver at the l-th snapshot ($l = 1, \ldots, n$) can be described by

$$\mathbf{X}_l = \beta\mathbf{a}_r(\varphi)\mathbf{a}_t^T(\theta)\mathbf{U} + \mathbf{V}_l, \tag{3}$$

where $\mathbf{a}_t(\theta) \in \mathbb{C}^{1\times q}$ and $\mathbf{a}_r(\varphi) \in \mathbb{C}^{1\times m}$ are the transmit and receive steering vectors and $\mathbf{V}_l \in \mathbb{C}^{m\times k}$ represents the noise term, which is a sum of contributions from thermal noise, clutter and jammer. Similar to [23]–[25], we assume it to be zero mean complex Gaussian, temporally white but spatially correlated with unknown covariance matrix. More specifically, the columns of $\mathbf{V}_l$ are independent complex Gaussian vectors with zeros mean and unknown covariance matrix $\mathbf{R}$. This thereby causes the covariance structure of the received signal to be indistinguishable between the signal-absent and -present cases. However, this problem could be solved by performing pulse compression:

$$\bar{\mathbf{X}}_l = \frac{1}{\sqrt{k}}\mathbf{X}_l\mathbf{U}^H = \sqrt{k}\beta\mathbf{a}_r(\varphi)\mathbf{a}_t^T(\theta) + \frac{1}{\sqrt{k}}\mathbf{V}_l\mathbf{U}^H. \tag{4}$$

Vectorizing $\bar{\mathbf{X}}_l$ gives

$$\mathbf{y}_l = \text{vec}(\bar{\mathbf{X}}_l) = \sqrt{k}\beta\mathbf{b}(\theta,\phi) + \mathbf{z}_l, \tag{5}$$

where $\mathbf{b}(\theta,\phi) = \mathbf{a}_t(\theta)\otimes\mathbf{a}_r(\varphi)$ and $\mathbf{z}_l = \frac{1}{\sqrt{k}}\text{vec}(\mathbf{V}_l\mathbf{U}^H)$. Therefore, the covariance matrix of the noise-only case is calculated as

$$\begin{aligned}\boldsymbol{\Sigma} = \mathbb{E}[\mathbf{z}_l\mathbf{z}_l^H] &= \frac{1}{k}\mathbb{E}[(\mathbf{U}^*\otimes\mathbf{I}_q)\text{vec}(\mathbf{V}_l)\text{vec}(\mathbf{V}_l)^H(\mathbf{U}^T\otimes\mathbf{I}_q)] \\ &= \frac{1}{k}(\mathbf{U}^*\mathbf{U}^T\otimes\mathbf{R}) \\ &= \mathbf{I}_q\otimes\mathbf{R}. \end{aligned} \tag{6}$$

When the target exists, this block-diagonal structure is destroyed, leading to $\boldsymbol{\Sigma} = \sqrt{k}\sigma_\beta^2\mathbf{b}(\theta,\phi)\mathbf{b}^H(\theta,\phi) + \mathbf{I}_q\otimes\mathbf{R}$, where $\sigma_\beta^2 = \mathbb{E}[|\beta|^2]$ is the variance of β. As a result, the hypothesis testing problem is summarized as[1]

$$\mathcal{H}_0 : \boldsymbol{\Sigma} = \mathbf{I}_q\otimes\mathbf{R} \tag{7a}$$

$$\mathcal{H}_1 : \boldsymbol{\Sigma} \succ \mathbf{I}_q\otimes\mathbf{R}, \tag{7b}$$

where $\mathbf{A}\succ\mathbf{B}$ is equivalent to $\mathbf{A}-\mathbf{B}$ being positive definite. With a total of n pulses transmitted, namely, n i.i.d. realizations of $\mathbf{y}$, the LMPIT in [1] can be adopted for the above hypothesis testing problem, which is

$$T_{\text{LMP}} = ||(\mathbf{I}_q\otimes\mathbf{S}_0)^{-\frac{1}{2}}\mathbf{S}(\mathbf{I}_q\otimes\mathbf{S}_0)^{-\frac{1}{2}}||_F^2, \tag{8}$$

where

$$\mathbf{S} = \sum_{i=1}^{n}\mathbf{y}_i\mathbf{y}_i^H \tag{9}$$

and $\mathbf{S}_0 = \text{Tr}(\mathbf{S})/q$.[2] Note that when $m = 1$, the LMPIT reduces to the John's test. Therefore, the John's test is the special case of the LMPIT.

Remark 1: Comparing with the independence test, the sphericity test further considers the identity of the diagonal blocks. In other words, it has utilized this additional information to enhance detection performance. When it comes to coherent MIMO radar detection, the temporary whiteness of the noise matches with this property, thereby suggesting that the sphericity test can utilize additional information to outperform the independence test in this scenario.

Remark 2: It should be noted that when the noise is spatially white but temporally correlated [16], the noise structure in (6) is still valid, provided that the receiver vectorizes $\mathbf{X}^T$ instead of $\mathbf{X}$. On the other hand, such a noise structure can also be found in other applications besides MIMO radar detection. For example, it follows from [19] that the noise structure of the "Two-Loop Vector" antenna array is $\mathbf{I}_2\otimes\boldsymbol{\Phi}$, with $\boldsymbol{\Phi}$ being a positive definite Hermitian matrix. Therefore, the LMPIT is not restricted to the coherent MIMO radar detection problem discussed above. On the other hand, the accuracy of the null distribution of LMPIT obtained in [1] can be further improved since the higher-order terms cannot be ignored for small sample situations. Also note that the non-null distribution of the LMPIT has not yet been studied in the literature. In the following we derive the accurate asymptotic null and non-null distributions for the LMPIT utilizing the asymptotic series expansion of the characteristic function of the LMPIT statistic. Besides, since [1] indicates that the LMPIT is in identical form for the real Gaussian observations, we also present its performance analysis in this case. However, the detailed derivations are only provided for the complex case as our current work focuses on target detection for MIMO radar.

III. Null Distribution

In this section, the asymptotic null distribution of T is obtained by performing the asymptotic expansion method. The

[1]When SNR is low, studying the rank structure of the signal covariance matrix does not further enhance detection performance [1]. Moreover, the steering vector may vary for diverse transmit/receive arrays, thus is not specifically exploited herein.

[2]Throughout this paper, the dimensions of all blocks are taken as $m\times m$

closed-form formula for threshold computation is derived as well.

Before applying the asymptotic expansion technique, the test statistic needs to be modified into a monotonic form which is asymptotically Chi-square distributed under the null hypothesis. As shown in [1], the following form of the LMPIT provides such a property:

$$T = n\mathrm{tr}\big((q\mathbf{S}(\mathbf{I}_q \otimes \mathrm{Tr}(\mathbf{S}))^{-1} - \mathbf{I}_p)^2\big). \tag{10}$$

The null distribution of T is provided in the following theorem:

Theorem 1: The null distribution of T can be approximated asymptotically up to $\mathbf{o}(n^{-2})$ by

$$\Pr(T \leqslant \gamma) = \sum_{k=0}^{3} h_k \Pr(\chi^2_{f+2k} \leqslant \gamma) + \mathbf{o}(n^{-2}), \tag{11}$$

where

$$h_0 = 1 + \frac{2m^3 - m}{12qn} - \frac{2p^3 - p}{12n} \tag{12a}$$

$$h_1 = \frac{p^3}{2n} - \frac{m^2 p}{2n} \tag{12b}$$

$$h_2 = \frac{p}{4n} - \frac{(2m^3 + m)}{4qn} + \frac{m^2 p}{n} - \frac{p^3}{2n} \tag{12c}$$

$$h_3 = \frac{m^3 + m}{3qn} - \frac{p}{3n} - \frac{m^2 p}{2n} + \frac{p^3}{6n}, \tag{12d}$$

$f = p^2 - m^2$ and χ^2_f denotes a Chi-squared distributed random variable with f DOFs.

Proof: The proof is given in Appendix A. ■

It follows from [11, (8.1-8.2)] that for the asymptotic distribution of T given in (11), its theoretical threshold for a given false-alarm rate P_{fa} is approximated as

$$\gamma(P_{\mathrm{fa}}) = u + \frac{2h_3 u}{f(f+2)(f+4)}\left[u^2 + (f+4)u + (f+2)(f+4)\right] + \frac{2h_2 u}{f(f+2)}(u + f + 2) + \frac{2h_1 u}{f} + \mathbf{o}\left(n^{-2}\right), \tag{13}$$

where $\Pr(\chi^2_f \leqslant u) = 1 - P_{\mathrm{fa}}$.

For the real-valued Gaussian case, the test statistic is modified as

$$T' = \frac{n}{2}\mathrm{tr}\big((q\mathbf{S}(\mathbf{I}_q \otimes \mathrm{Tr}(\mathbf{S}))^{-1} - \mathbf{I}_p)^2\big), \tag{14}$$

whose null distribution is given by the following theorem.

Theorem 2: The null distribution of T' can be approximated asymptotically up to $\mathbf{o}(n^{-2})$ by

$$\Pr(T' \leqslant \gamma) = \sum_{k=0}^{3} h'_k \Pr(\chi^2_{f'+2k} \leqslant \gamma) + \mathbf{o}(n^{-2}), \tag{15}$$

where $f' = (p^2 + p - m^2 - m)/2$ and

$$h'_0 = 1 - \frac{2p^3 + 3p^2 - p}{24n} + \frac{2m^3 + 3m^2 - m}{24qn} \tag{16a}$$

$$h'_1 = -\frac{(p+1)(m^2 + m - p^2 - p)}{4n} \tag{16b}$$

$$h'_2 = \frac{-2m^2 p - 5mp + 4p^3 + 6p^2 - 5p}{8q^2 n} + \frac{4p^2 + 6p}{8qn} - \frac{2p^3 + 5p^2 + p}{8n} \tag{16c}$$

$$h'_3 = \frac{2m^2 p + 6mp - 3p^3 - 6p^2 + 8p}{12q^2 n} - \frac{3p^2 + 6p}{12qn} + \frac{p^3 + 3p^2 - 2p}{12n}. \tag{16d}$$

On the basis of this result, the LMPIT could be applied in other fields besides MIMO radar. But the proof is omitted for its similarity to that of the complex case. ■

Remark 3: The result of [11, Th. 5.1] is the special case of Theorem 2 at $m = 1$. However, when setting $m = 1$, our result does not reduce to that in [11]. As shown by simulations in [27], our result turns out to be more accurate. This is because there are errors in the formulas in [11]. That is, the terms $436/(24p)$, $-216/(4p)$, $420/(8p)$ and $-200/(12p)$ in (5.3) of [11] should be corrected as $1/(6p)$, 0, $-3/(2p)$, $4/(3p)$, respectively.

Remark 4: Given all positive integer moments of a detector, the Box's approximation [28], [29] expands its null distribution to a more accurate $\mathbf{o}(n^{-3})$, by performing a comparatively simpler calculation. Therefore, when analysing the null distributions of GLRTs, the Box's approximation is preferable since the exact moments are usually inferrable. On the contrary, for LMPITs, it is normally impossible to derive all these moments. Thus the proposed asymptotic expansion method should be applied.

IV. Non-Null Distribution Under Close Hypotheses

In this section, we derive the distribution of T under the non-null hypothesis: $\mathbf{\Sigma} = \sqrt{k}\sigma^2_\beta \mathbf{b}(\theta,\phi)\mathbf{b}^H(\theta,\phi) + \mathbf{I}_q \otimes \mathbf{R}$. To facilitate our computations, we utilize the property that the distribution of T remains invariant when $\mathbf{\Sigma}$ is pre- and post-multiplied by a block spherical matrix and define

$$\mathbf{\Sigma}' = (\mathbf{I}_q \otimes \mathrm{Tr}(\mathbf{\Sigma})/q)^{-1/2}\mathbf{\Sigma}(\mathbf{I}_q \otimes \mathrm{Tr}(\mathbf{\Sigma})/q)^{-1/2}. \tag{17}$$

When the non-zero elements of $(\mathbf{\Sigma}' - \mathbf{I}_p)$ are of order $\mathbf{o}(1/\sqrt{n})$, the alternative hypothesis is considered to be "close" to the null hypothesis. Under such circumstances, the distribution of T is given in the following theorem:

Theorem 3: Under the alternative hypothesis, the distribution of T can be approximated asymptotically up to $\mathbf{o}(n^{-\frac{3}{2}})$

by

$$\Pr(T \leqslant \gamma) = \sum_{k=0}^{6} g_k \Pr(\chi^2_{f+2k}(a_2) \leqslant \gamma) + \sum_{k=0}^{3} h_k \Pr(\chi^2_{f+2k}(a_2) \leqslant \gamma) + \mathbf{o}\left(n^{-\frac{3}{2}}\right), \quad (18)$$

where

$$g_0 = \frac{2a_3}{3\sqrt{n}} + \frac{e_2}{2qn} + \frac{2a_3^2}{9n} - \frac{3a_4}{4n} \quad (19a)$$

$$g_1 = -\frac{a_3}{\sqrt{n}} + \frac{b_2}{2qn} - \frac{3e_2}{2qn} + \frac{3a_4}{2n} - \frac{2a_3^2}{3n} \quad (19b)$$

$$g_2 = \frac{a_3^2}{2n} + \frac{e_2}{2qn} + \frac{a_2 p}{2n} \quad (19c)$$

$$g_3 = \frac{a_3}{3\sqrt{n}} + \frac{b_2}{2qn} + \frac{e_2}{qn} + \frac{a_2 m}{qn} - \frac{a_4}{n} - \frac{a_2 p}{n} + \frac{2a_3^2}{9n} \quad (19d)$$

$$g_4 = -\frac{a_3^2}{3n} - \frac{b_2}{qn} - \frac{a_2 m}{qn} - \frac{a_4}{4n} + \frac{pa_2}{2n} \quad (19e)$$

$$g_5 = \frac{a_4}{2n} - \frac{e_2}{2qn} \quad (19f)$$

$$g_6 = \frac{a_3^2}{18n} \quad (19g)$$

with $\mathbf{Z} \triangleq \sqrt{n}(\mathbf{\Sigma}' - \mathbf{I}_p)$, $a_i = \text{tr}(\mathbf{Z}^i)$, $b_2 = \sum_{i,j=1}^{q} |\text{tr}(\mathbf{Z}_{ij})|^2$ and $e_2 = \text{tr}(\text{Tr}(\mathbf{Z}^2)^2)$ and $\chi_f^2(\sigma^2)$ denoting a noncentral Chi-squared distribution with f DOFs and noncentrality parameter σ^2.

Proof: The proof is given in Appendix B. ■

It is seen that if we set $\mathbf{\Sigma}$ to be the identity matrix, the same asymptotic series expansion of the null distribution as (11) is obtained. Following the same procedure, the result for the real-valued Gaussian case is also derived, which is provided in the following theorem:

Theorem 4: Under the alternative hypothesis, the distribution of T can be approximated asymptotically up to $\mathbf{o}(n^{-\frac{3}{2}})$ by

$$\Pr(T \leqslant \gamma) = \sum_{k=0}^{6} g'_k \Pr(\chi^2_{f'+2k}(a_2/2) \leqslant \gamma) + \sum_{k=0}^{3} h'_k \Pr(\chi^2_{f'+2k}(a_2/2) \leqslant \gamma) + \mathbf{o}\left(n^{-\frac{3}{2}}\right), \quad (20)$$

where

$$g'_0 = \frac{a_3}{3\sqrt{n}} + \frac{e_2}{4qn} + \frac{a_3^2}{18n} - \frac{3a_4}{8n} \quad (21a)$$

$$g'_1 = -\frac{a_3}{2\sqrt{n}} + \frac{f_2}{4qn} + \frac{b_2}{4qn} - \frac{3e_2}{4qn} + \frac{3a_4}{4n} - \frac{a_3^2}{6n} \quad (21b)$$

$$g'_2 = \frac{a_3^2}{8n} + \frac{e_2}{4qn} + \frac{(p+1)a_2}{4n} \quad (21c)$$

$$g'_3 = \frac{a_3}{6\sqrt{n}} + \frac{f_2}{4qn} + \frac{b_2}{4qn} + \frac{e_2}{2qn} + \frac{(m+1)a_2}{2qn} - \frac{a_4}{2n} - \frac{(2p+3)a_2}{4n} + \frac{a_3^2}{18n} \quad (21d)$$

$$g'_4 = \frac{(p+2)a_2}{4n} - \frac{a_3^2}{12n} - \frac{f_2}{2qn} - \frac{b_2}{2qn} - \frac{(m+1)a_2}{2qn} - \frac{a_4}{8n} \quad (21e)$$

$$g'_5 = \frac{a_4}{4n} - \frac{e_2}{4qn} \quad (21f)$$

$$g'_6 = \frac{a_3^2}{72n} \quad (21g)$$

with $f_2 = \sum_{i,j=1}^{q} \text{tr}(\mathbf{Z}_{ij}^2)$.

Analogously to Theorem 2, the proof of Theorem 4 is omitted. ■

V. Non-Null Distribution Under Far Hypothesis

When $\mathbf{\Sigma}'$ is not that close to the identity matrix, the results in Section IV become invalid. Therefore, it is necessary to derive a new approximation to the non-null distribution for high SNR case. Here, we resort to the so-called "moment-matching" method [7], [8], [30], [31], namely, first evaluating the mean and variance of T and then matching them with those of a known distribution with the same support.

The exact formulas for moments are difficult to obtain. However, we may resort to the "asymptotic expansion method" to acquire simple but accurate moment expressions. In doing so, approximate representations of mean and variance of T are established and given in the following theorem.

Theorem 5: For large n and small p, the mean and variance of T can be respectively approximated as: [3]

$$u = \mathbb{E}[T] = n\text{tr}(\mathbf{Z}'^2) + e_0(\mathbf{\Sigma}') + \mathbf{o}(n^{-\frac{1}{2}}) \quad (22a)$$

$$v = \mathbb{E}[(T-u)^2] = ne_1(\mathbf{\Sigma}') + \mathbf{o}(1), \quad (22b)$$

where

$$e_0(\mathbf{\Sigma}') = \text{tr}(\mathbf{\Sigma})^2 - \frac{2}{q}\sum_{i,j=1}^{q} \text{tr}(\mathbf{\Sigma}_{ij})\text{tr}((\mathbf{\Sigma}^2 + \mathbf{Z\Sigma})_{ji}) + \frac{2}{q^2}\sum_{i,j,k=1}^{q} \text{tr}(\mathbf{\Sigma}_{ij})\text{tr}((\mathbf{Z\Sigma})_{kk}\mathbf{\Sigma}_{ji}) + \frac{1}{q^2}\sum_{i,j,k,l=1}^{q} |\text{tr}(\mathbf{\Sigma}_{ij}\mathbf{\Sigma}_{kl})|^2 \quad (23a)$$

$$e_1(\mathbf{\Sigma}') = 4\text{tr}\big((\mathbf{Z\Sigma})^2\big) - \frac{8}{q}\text{tr}\big(\text{Tr}(\mathbf{\Sigma Z \Sigma})\text{Tr}(\mathbf{Z\Sigma})\big) + \frac{4}{q^2}\text{tr}\big(\text{Tr}\big(\mathbf{Z\Sigma}\big)\text{Tr}\big(\mathbf{\Sigma}(\mathbf{I}_q \otimes \text{Tr}(\mathbf{Z\Sigma}))\mathbf{\Sigma}\big)\big) \quad (23b)$$

[3]Equivalently, the approximation error for the standard deviation is of order $n^{-\frac{1}{2}}$, which is the same as that of mean value. Thus the $\mathbf{o}(1)$ terms can be omitted for the variance.

and

$$\mathbf{Z}' \triangleq \mathbf{\Sigma}' - \mathbf{I}_p. \tag{24}$$

Proof: The proof is given in Appendix C. ■

Motivated by the fact that $T \in (0, +\infty)$, we choose the Gamma distribution, which has the same support as T, to approximate its non-null distribution. By matching the mean and variance of a Gamma random variable to those of T we have the following theorem.

Theorem 6: For large n and small p, the two-first-moment Gamma approximation to the non-null distribution of T is

$$p(T < \gamma) \approx \int_{-\inf}^{\gamma} \frac{y^{\alpha-1}\beta^{-\alpha}e^{-\frac{y}{\beta}}}{\Gamma(\alpha)}dy, \tag{25}$$

where

$$\alpha = \frac{u^2}{v}, \quad \beta = \frac{v}{u}. \tag{26}$$

Proof: For a Gamma random variable x with density function (25), its mean and variance are given by

$$u = \alpha\beta, \quad v = \alpha\beta^2. \tag{27}$$

Matching its mean and variance with those of T and solving (27), (26) is obtained. This completes the proof. ■

VI. Simulation Results

In this section, we first carry out numerical simulations to validate our theoretical computations of the false-alarm and detection probabilities, as well as decision threshold. Then we illustrate the detection performance of the LMPIT in unknown colored noise. Each result represents an average of 10^6 Monte Carlo trials.

We consider a coherent MIMO radar system with uniform linear arrays at both transmitter and receiver sides, in which the inter-antenna spacings are equally taken as half-wavelength. The transmitted waveforms are orthogonal quadrature phase shift keyed (QPSK) sequences with length 64. The reflection factor β is modeled as complex Gaussian variable with zero mean and variance σ_β^2. The spatially correlated noise is a complex Gaussian vector with a Toeplitz covariance matrix $\mathbf{R}$ whose first row is $[\sigma_n^2, \sigma_n^2\rho, \cdots, \sigma_n^2\rho^{p-1}]$, namely, the correlations among antennas follow an exponential decay model. Recall that under the alternative hypothesis, the covariance matrix of the output data, after pulse compression, is $\mathbf{\Sigma} = \sqrt{k}\sigma_\beta^2\mathbf{b}(\theta,\phi)\mathbf{b}^H(\theta,\phi) + \mathbf{I}_q \otimes \mathbf{R}$. The SNR (in dB) is defined as

$$\text{SNR} = 10\log_{10}\frac{\text{tr}(\mathbf{\Sigma}) - q\text{tr}(\mathbf{R})}{q\text{tr}(\mathbf{R})} = 10\log_{10}\frac{\sqrt{k}\sigma_\beta^2}{\sigma_n^2}. \tag{28}$$

To quantify the approximation error between the theoretical and simulated cumulative distribution functions (CDFs), we employ the Cramér-von Mises goodness-of-fit test, which is defined as [32]:

$$\epsilon = \frac{1}{Q}\sum_{i=1}^{Q}\left|G(x_i) - \hat{G}(x_i)\right|^2. \tag{29}$$

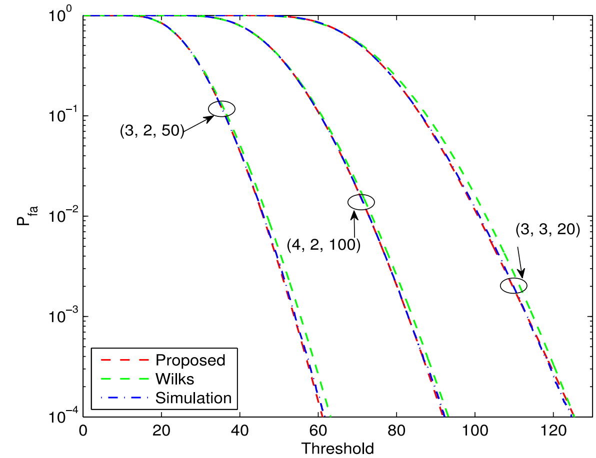

Fig. 1. False-alarm probability versus threshold for different values of (m, q, n).

Here $G(x_i)$ is the distribution determined by simulation, which is taken as the theoretical value, $\hat{G}(x_i)$ is its estimate obtained by our derived approximation and $Q = 10^4$.

A. Null Distribution

In Fig. 1, the false-alarm probabilities are plotted as functions of threshold for (m, q, n) values of $(3, 3, 20)$, $(3, 2, 50)$ and $(4, 2, 100)$. For the purpose of comparison, we also present the results obtained by the Wilks' theorem in [1], that is

$$T \sim \chi_f^2. \tag{30}$$

It is indicated in Fig. 1 that the proposed approximation surpasses previous result by Wilks' theorem in terms of fitting their simulated counterparts. In addition, the approximation errors measured by (29) are given as $[8.59, 0.116, 0.0592] \times 10^{-5}$ for Wilks' approximation and $[3.29, 0.362, 0.105] \times 10^{-7}$ for proposed approximation. Thus, our derived formula is able to provide more precise approximations than previous result obtained from Wilks' theorem.

B. Decision Threshold

Fig. 2 shows the actual P_{fa} corresponding to the calculated threshold value versus prescribed P_{fa} under parameter settings $(m, q, n) = (4, 2, 100)$. It is seen that our threshold formula can yield a P_{fa} that aligns very well with the prescribed value. In contrast, the Wilks' approximation has a quite large gap between the actual and prescribed false-alarm probabilities, which in turn implies that the second-order terms of the asymptotic series expansion can provide an important correction for the previous results in [1], particularly for small sample conditions.

Table I lists the exact and approximate threshold value for false-alarm rates 0.01 and 0.001. It is seen that our approximations with the second-order term are able to provide threshold values which are much closer to the exact ones than Wilks' result. This also confirms that (13) can provide reasonably accurate thresholds.

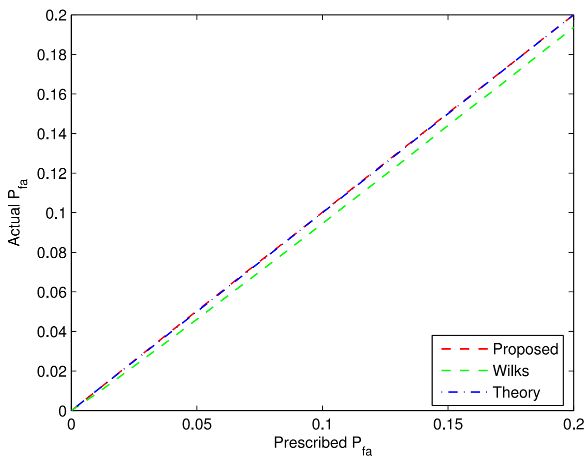

Fig. 2. Analytical threshold selection: prescribed P_{fa} versus actual P_{fa} at $m = 4$, $q = 2$ and $n = 100$.

TABLE I
THRESHOLD APPROXIMATIONS FOR DIFFERENT FALSE-ALARM PROBABILITIES AT $m = 4$, $q = 2$ AND $n = 100$

P_{fa}	Proposed	Wilks	Simulation
0.01	72.9568	73.6826	73.0164
0.001	83.0533	84.0371	83.0626

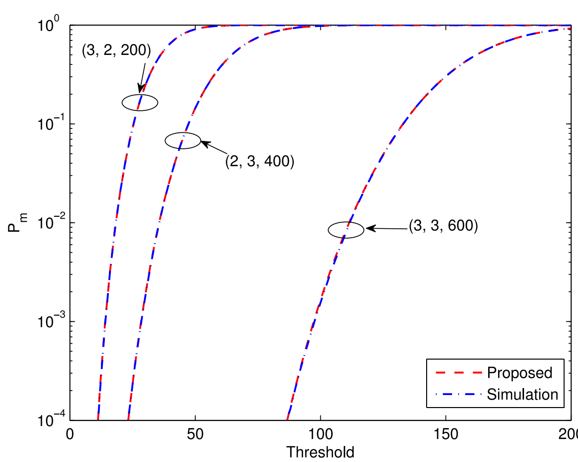

Fig. 3. Detection probability versus threshold for $\mathrm{SNR} = -11$ dB and different values of (m, q, n).

C. Non-Null Distribution

We now study the precision of the derived detection probability formulas. Here we first examine the accuracy of (18), which is derived for the low SNR case. Accordingly, in Fig. 3, we assume there is one source at $(\theta, \phi) = (\pi/6, -\pi/4)$, whose SNR is -11 dB and (m, q, n) are set to be $(3, 2, 200)$, $(2, 3, 400)$ and $(3, 3, 600)$. It is seen that the proposed approximations are very accurate in terms of fitting the simulated ones. More precisely, the approximate errors equal $[0.264, 0.811, 2.00] \times 10^{-7}$.

In Fig. 4, the SNR is changed to -2 dB, which suggests (25) should be used here. The error between the approximate and simulated detection probabilities are $[1.05, 0.250, 0.374] \times 10^{-5}$.

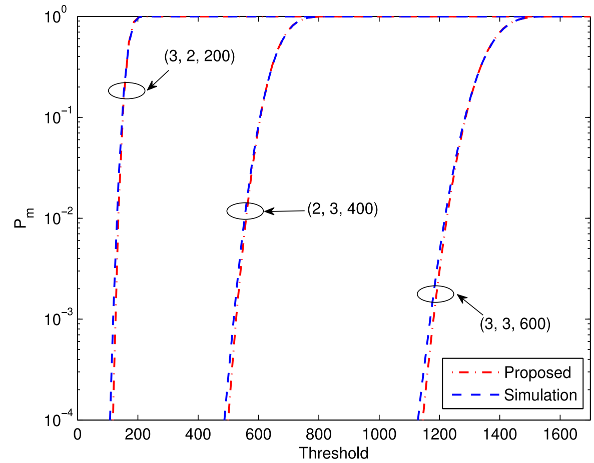

Fig. 4. Detection probability versus threshold for $\mathrm{SNR} = -2$ dB and different values of (m, q, n).

These results imply that the derived non-null distribution formulas are able to accurately predict the detection performance of the LMPIT approach for both high and low SNR cases.

D. Detection Performance

Let us now investigate the detection power and robustness of the LMPIT in the presence of spatially correlated noise. For comparison purpose, another blind-noise-statistics detector, namely, the Wilks' detector [17], [34] is considered[4], which is defined as

$$T_W = \frac{|\hat{\mathbf{R}}|}{|\hat{\mathbf{R}} + \hat{\mathbf{\Sigma}}|}, \tag{31}$$

where

$$\hat{\mathbf{R}} = \frac{1}{l}\mathbf{W}\mathbf{W}^H \tag{32}$$

$$\hat{\mathbf{\Sigma}} = \frac{1}{n}\sum_{j=1}^{n}\bar{\mathbf{X}}_j\bar{\mathbf{X}}_j^H \tag{33}$$

with $\mathbf{W} \in \mathbb{C}^{p\times l}$ being the noise-only secondary data matrix , which is independent of $\bar{\mathbf{X}}$. In addition, it is worthwhile to study the performance of the GLRT and LMPIT for independence [1] in MIMO radar detection, whose definitions are respectively given as:

$$T_{\mathrm{GLR}} = \frac{|\mathbf{S}|}{|\mathrm{Tr}(\mathbf{S})|^q} \tag{34}$$

$$T_{\mathrm{I}} = ||\mathbf{S}\mathbf{S}_D^{-1}||_F^2, \tag{35}$$

where $\mathbf{S}_D = \mathrm{diag}(\mathbf{S}_{11}, \cdots, \mathbf{S}_{qq})$.

In Fig. 5, the detection probabilities are plotted as a function of pulse number n, where the false alarm rate is fixed at 0.001 and other parameters are set as $m = q = 3$, $\mathrm{SNR} = -10$ dB and $(\theta, \phi) = (\pi/3, \pi/4)$. The noise correlation factor ρ is set to be 0 and 0.3 in Fig. 5(a) and (b), respectively. In addition, $l = n$

[4]Since [12], [13], [15], [16] adopt the Swerling-I model, it is not able to compare their performances with the LMPIT.

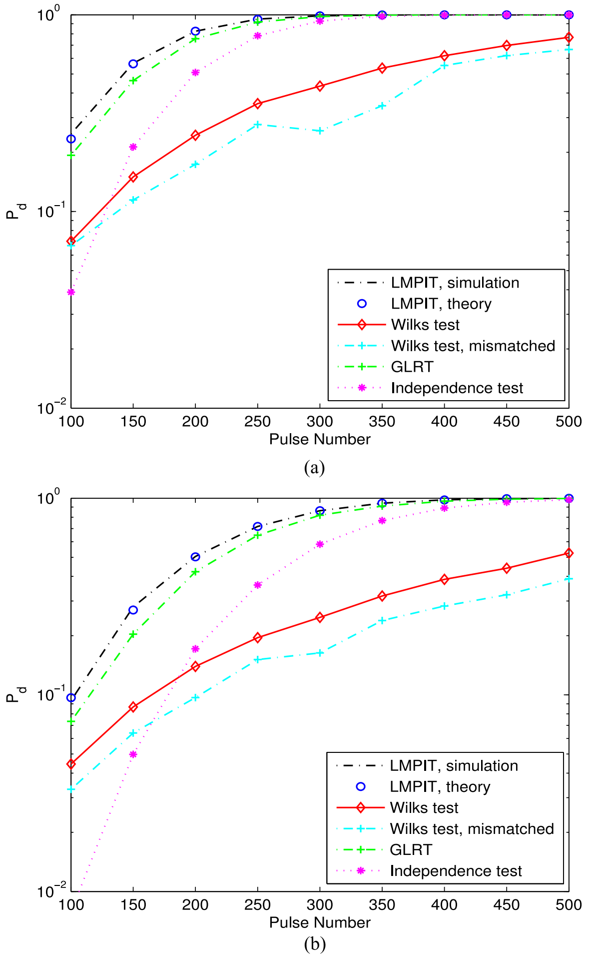

Fig. 5. Performance comparison for different number of pulses at $m = 3$, $q = 3$ and SNR $= -10$ dB. (a) $\rho = 0$, $\rho' = 0.2$. (b) $\rho = 0.3$, $\rho' = 0.4\exp(0.1\imath\pi)$.

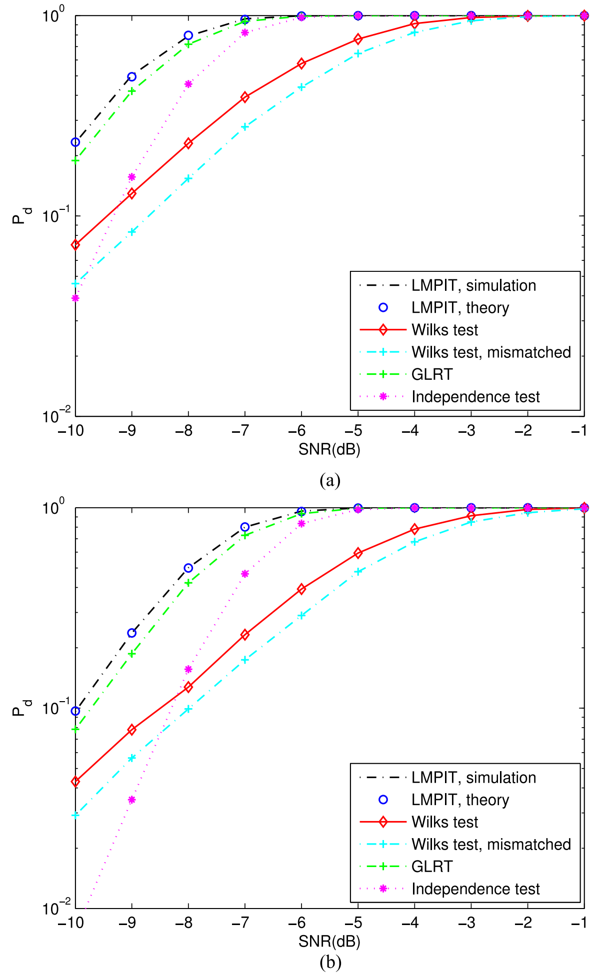

Fig. 6. Performance comparison for different SNRs at $m = 3$, $q = 3$, $n = 100$ and $l = 100$. (a) $\rho = 0$, $\rho' = 0.2$. (b) $\rho = 0.3$, $\rho' = 0.4\exp(0.1\imath\pi)$.

noise-only observations are collected for the Wilks' test. We consider two cases: 1) the secondary data possess identical noise covariance matrix as the primary data, and 2) there is a mismatch between the secondary and primary data, in which the noise correlation factor ρ' is set as 0.2 in Fig. 5(a) and $0.4\exp(0.1\imath\pi)$ in Fig. 5(b). It is seen that the LMPIT outperforms GLRT, independence test and Wilks' test, and the detection probability of Wilks' test decreases when the secondary data do not share the same noise covariance structure as the primary data.

In Fig. 6, SNR is taken as the independent variable while n and l are both fixed at 100 with other parameters being unchanged. Again, the detection probability of LMPIT is higher than that of the other three detectors. It is also observed that as ρ increases from 0 to 0.3, the performance of LMPIT does not change obviously. This indicates that the LMPIT is robust against spatially colored noise in the coherent MIMO radar detection. On the other hand, it does not require additional noise-only secondary data, thereby being free from the mismatch problem. This is because it exploits the block-spherical structure of noise covariance matrix which is ignored by the Wilks' detection approach. Besides, GLRT and the independence test also exhibit robustness against colored noise, but its detection power is inferior to the LMPIT in coherent MIMO radar since the later is optimal in the low SNR regime.

VII. Conclusion

In this work, we have derived the asymptotic formulas for the distributions of the LMPIT for sphericity of Gaussian vectors in real- and complex-valued situations, ending up with accurate null and non-null distributions as well as closed-form expressions for the decision threshold. More specifically, by inverting the asymptotic series expansion of the characteristic function of the LMPIT statistic, the null distribution is expressed as function of Chi-squared distributions. Meanwhile, the non-null distribution is derived in terms of weighted sum of non-central Chi-squared distributions. The convergence rates are $\mathbf{o}(n^{-2})$ and $\mathbf{o}(n^{-\frac{3}{2}})$ for the null and non-null hypotheses, respectively. Extensive numerical results validate the accuracies of the derived asymptotic distributions and analytical threshold formula.

Appendix A
Proof of Theorem 1

Proof: Setting $\mathbf{Y} = \sqrt{n}\log(\mathbf{S}/n)$ as in [26], T can be expressed in terms of $\mathbf{Y}$ as:

$$T = u_0(\mathbf{Y}) + \frac{1}{\sqrt{n}}u_1(\mathbf{Y}) + \frac{1}{n}u_2(\mathbf{Y}) + \mathbf{o}(n^{-\frac{3}{2}}), \qquad (36)$$

where

$$u_0(\mathbf{Y}) = \text{tr}(\mathbf{Y}^2) - \frac{1}{q}\text{tr}(\text{Tr}(\mathbf{Y})^2) \tag{37a}$$

$$u_1(\mathbf{Y}) = \text{tr}(\mathbf{Y}^3) + \frac{2}{q^2}\text{tr}(\text{Tr}(\mathbf{Y})^3) - \frac{3}{q}\text{tr}(\text{Tr}(\mathbf{Y})\text{Tr}(\mathbf{Y}^2)) \tag{37b}$$

$$\begin{aligned} u_2(\mathbf{Y}) = &\frac{7}{12}\text{tr}(\mathbf{Y}^4) - \frac{3}{q^3}\text{tr}(\text{Tr}(\mathbf{Y})^4) - \frac{7}{3q}\text{tr}(\text{Tr}(\mathbf{Y})\text{Tr}(\mathbf{Y}^3)) \\ &- \frac{5}{4q}\text{tr}(\text{Tr}(\mathbf{Y}^2)^2) + \frac{1}{q^2}\text{tr}((\mathbf{Y}(\mathbf{I}_q \otimes \text{Tr}(\mathbf{Y})))^2) \\ &+ \frac{5}{q^2}\text{tr}(\text{Tr}(\mathbf{Y})^2\text{Tr}(\mathbf{Y}^2)). \end{aligned} \tag{37c}$$

The proof of (36) is given in Appendix D. Without loss of generality, we set $\mathbf{\Sigma} = \mathbf{I}_p$, yielding $\mathbf{S} \sim \mathcal{CW}_p(n, \mathbf{I}_p)$. It follows from [26, eq. (13)] that the asymptotic distribution of $\mathbf{Y}$ under large n is

$$\begin{aligned} f_{\mathbf{Y}}(\mathbf{Y}) = c\,\text{etr}\left(-\frac{\mathbf{Y}^2}{2}\right) \times \Bigg[1 - \frac{\text{tr}(\mathbf{Y}^3)}{6\sqrt{n}} - \frac{\text{tr}^2(\mathbf{Y})}{12n} + \frac{p\text{tr}(\mathbf{Y}^2)}{12n} \\ -\frac{\text{tr}(\mathbf{Y}^4)}{24n} + \frac{\text{tr}^2(\mathbf{Y}^3)}{72n} + \mathbf{o}(n^{-\frac{3}{2}})\Bigg], \end{aligned} \tag{38}$$

where

$$c = \frac{N^{p(N-\frac{p}{2})}\pi^{-\frac{p(p-1)}{2}}}{\prod_{k=1}^{p}(\Gamma(n+1-k))} \times \exp(-np). \tag{39}$$

Using (38) and performing straightforward manipulations, we write the characteristic function of T as

$$\begin{aligned} C_T(t) = c\int \exp\left(-\frac{1}{2}\text{tr}(\mathbf{Y}^2) + (it)u_0(\mathbf{Y})\right) \\ \times \Bigg[1 + \frac{1}{n}\Bigg\{\frac{p\text{tr}(\mathbf{Y}^2)}{12} - \frac{\text{tr}^2(\mathbf{Y})}{12} - \frac{\text{tr}(\mathbf{Y}^4)}{24} + (it)u_2(\mathbf{Y}) \\ +\frac{1}{2}\left((it)u_1(\mathbf{Y}) - \frac{1}{6}\text{tr}(\mathbf{Y}^3)\right)^2\Bigg\} + \mathbf{o}(n^{-\frac{3}{2}})\Bigg]\,d\mathbf{Y}. \end{aligned} \tag{40}$$

The key to solving (40) is to express the exponential term in terms of Gaussian probability density function (PDF), which can be unfolded as

$$\begin{aligned} &-\frac{1}{2}\text{tr}(\mathbf{Y}^2) + (it)u_0(\mathbf{Y}) \\ &= -\frac{1-2it}{2}\Bigg(\sum_{j=1}^{p}\mathbf{Y}_{j,j}^2 + 2\sum_{\substack{j,k=1\\ j<k}}^{p}\left((\mathbf{Y}_{j,k}^R)^2 + (\mathbf{Y}_{j,k}^I)^2\right) \\ &+ \frac{2it}{(1-2it)q}\sum_{r,s}^{q}\Bigg[\sum_{j=1}^{m}(\mathbf{Y}_{rr})_{j,j}(\mathbf{Y}_{ss})_{j,j} \\ &+ 2\sum_{\substack{j,k=1\\ j<k}}^{m}\left((\mathbf{Y}_{rr})_{j,k}^R(\mathbf{Y}_{ss})_{j,k}^R + (\mathbf{Y}_{rr})_{j,k}^I(\mathbf{Y}_{ss})_{j,k}^I\right)\Bigg]\Bigg). \end{aligned} \tag{41}$$

It is observed that the parameters of $\mathbf{Y}$ are not separable. Therefore, we cannot assume them to be independently distributed Gaussian variables as in [26]. To proceed, we define $\tilde{\mathbf{y}}_1 \in \mathbb{R}^{1\times p}$, $\tilde{\mathbf{y}}_2 \in \mathbb{R}^{1\times(mp-p)}$ and $\tilde{\mathbf{y}}_3 \in \mathbb{R}^{1\times(p^2-mp)}$ as

$$\begin{aligned} \tilde{\mathbf{y}}_1 = [&(\mathbf{Y}_{11})_{1,1}, \cdots, (\mathbf{Y}_{qq})_{1,1}, \cdots, (\mathbf{Y}_{11})_{2,2}, \cdots, (\mathbf{Y}_{qq})_{2,2}, \\ &\cdots, (\mathbf{Y}_{11})_{m,m}, \cdots, (\mathbf{Y}_{qq})_{m,m}] \\ \tilde{\mathbf{y}}_2 = [&(\mathbf{Y}_{11})_{1,2}^R, \cdots, (\mathbf{Y}_{qq})_{1,2}^R, (\mathbf{Y}_{11})_{1,3}^R, \cdots, (\mathbf{Y}_{qq})_{1,3}^R, \cdots, \\ &(\mathbf{Y}_{11})_{m-1,m}^R, \cdots, (\mathbf{Y}_{qq})_{m-1,m}^R, (\mathbf{Y}_{11})_{1,2}^I, \cdots, \\ &(\mathbf{Y}_{qq})_{1,2}^I, (\mathbf{Y}_{11})_{1,3}^I, \cdots, (\mathbf{Y}_{qq})_{1,3}^I, \cdots, (\mathbf{Y}_{11})_{m-1,m}^I, \\ &\cdots, (\mathbf{Y}_{qq})_{m-1,m}^I] \\ \tilde{\mathbf{y}}_3 = [&(\mathbf{Y}_{12})_{1,2}^R, (\mathbf{Y}_{12})_{1,3}^R, \cdots, (\mathbf{Y}_{12})_{m-1,m}^R, \cdots, (\mathbf{Y}_{(q-1)q})_{1,2}^R, \\ &(\mathbf{Y}_{(q-1)q})_{1,3}^R, \cdots, (\mathbf{Y}_{(q-1)q})_{m-1,m}^R, (\mathbf{Y}_{12})_{1,2}^I, (\mathbf{Y}_{12})_{1,3}^I, \\ &\cdots, (\mathbf{Y}_{12})_{m-1,m}^I, \cdots, (\mathbf{Y}_{(q-1)q})_{1,2}^I, (\mathbf{Y}_{(q-1)q})_{1,3}^I, \cdots, \\ &(\mathbf{Y}_{(q-1)q})_{m-1,m}^I] \end{aligned} \tag{42}$$

and set $\tilde{\mathbf{y}} = [\tilde{\mathbf{y}}_1, \tilde{\mathbf{y}}_2, \tilde{\mathbf{y}}_3]$. Therefore, the problem is converted into searching matrix $\mathbf{\Gamma}$ such that

$$\tilde{\mathbf{y}}\mathbf{\Gamma}^{-1}\tilde{\mathbf{y}}^H = (1-2it)\left(\text{tr}(\mathbf{Y}^2) + \frac{2it}{(1-2it)q}\text{tr}(\text{Tr}(\mathbf{Y})^2)\right). \tag{43}$$

Combining (41), (42) and (43), we obtain

$$\mathbf{\Gamma} = \begin{bmatrix} \mathbf{I}_m \otimes \mathbf{\Delta} & \mathbf{0}_{p\times(mp-p)} & \mathbf{0}_{p\times(p^2-mp)} \\ \mathbf{0}_{(mp-p)\times p} & \frac{1}{2}\mathbf{I}_{m^2-m} \otimes \mathbf{\Delta} & \mathbf{0}_{(p^2-mp)\times(mp-p)} \\ \mathbf{0}_{(p^2-mp)\times p} & \mathbf{0}_{(mp-p)\times(p^2-mp)} & \frac{\phi}{2}\mathbf{I}_{p^2-mp} \end{bmatrix}, \tag{44}$$

where

$$\mathbf{\Delta} = \begin{bmatrix} \phi+\sigma & \sigma & \dots & \sigma \\ \sigma & \phi+\sigma & \dots & \sigma \\ \vdots & \vdots & \ddots & \vdots \\ \sigma & \sigma & \dots & \phi+\sigma \end{bmatrix} \tag{45}$$

with $\phi = (1-2it)^{-1}$ and $\sigma = (1-\phi)/q$. To this end, we have expressed the exponential term in (40) as $\exp(-\tilde{\mathbf{y}}\mathbf{\Gamma}^{-1}\tilde{\mathbf{y}}^H)$. It is thereby reasonable to take the integration in (40) as the expectation over $\tilde{\mathbf{y}} = \mathbf{w}\mathbf{\Gamma}^{\frac{1}{2}}$, where $\mathbf{w} \in \mathbb{R}^{1\times p^2}$ has mutually independent standard Gaussian entries. Consequently, the characteristic function can be expressed as:

$$\begin{aligned} C_T(t) = c_1\phi^{\frac{f}{2}}\mathbb{E}\Bigg[1 + \frac{1}{n}\Bigg\{\frac{p\text{tr}(\mathbf{Y}^2)}{12} \\ - \frac{\text{tr}^2(\mathbf{Y})}{12} - \frac{\text{tr}(\mathbf{Y}^4)}{24} + (it)u_2(\mathbf{Y}) \\ + \left((it)u_1(\mathbf{Y}) - \frac{1}{6}\text{tr}(\mathbf{Y}^3)\right)^2\Bigg\} + \mathbf{o}(n^{-\frac{3}{2}})\Bigg]. \end{aligned} \tag{46}$$

Herein, $f = p^2 - m^2$ and $c_1 = c \times (2\pi)^{\frac{p^2}{2}} 2^{-\frac{p(p-1)}{2}}$, which could be replaced by its Stirlings approximation [26]

$$c_1 = 1 - \frac{2p^3 - p}{12n} + \mathbf{o}\left(n^{-2}\right). \tag{47}$$

Moreover, note that the odd moments of Y in (46) are zero and thereby can be omitted, while the non-zero expectations in (46) are listed in Table II of Appendix E.

Combining (46), (47) and Table II, we obtain the asymptotic expression of the characteristic function:

$$C_T(t) = \phi^{\frac{f}{2}} \left[\sum_{k=0}^{3} h_k \phi^k + \mathbf{o}\left(n^{-2}\right)\right], \tag{48}$$

where

$$h_0 = 1 + \frac{2m^3 - m}{12qn} + \frac{-2p^3 + p}{12n} \tag{49a}$$

$$h_1 = \frac{p^3}{2n} - \frac{m^2 p}{2n} \tag{49b}$$

$$h_2 = \frac{p}{4n} - \frac{(2m^3 + m)}{4qn} + \frac{m^2 p}{n} - \frac{p^3}{2n} \tag{49c}$$

$$h_3 = \frac{m^3 + m}{3qn} - \frac{p}{3n} - \frac{m^2 p}{2n} + \frac{p^3}{6n} \tag{49d}$$

with $\phi = (1 - 2it)^{-1}$ as defined after (45). Note that the order of remaining terms reduces to $\mathbf{o}(n^{-2})$ due to the fact that the $\mathbf{o}(n^{-\frac{3}{2}})$ terms contain only odd moments of $\mathbf{Y}$ which equal zero. Inverting the characteristic function yields (11). This completes the proof of Theorem 1. ■

Appendix B
Proof of Theorem 3

Proof: It is proved in [26] that in the low SNR case, the asymptotic distribution of $\mathbf{Y}$ is determined by

$$f_{\mathbf{Y}}(\mathbf{Y}) = c\,\mathrm{etr}(v_0) \left[1 + \frac{v_1(\mathbf{Y})}{\sqrt{n}} + \frac{v_2(\mathbf{Y})}{n} + \frac{v_1^2(\mathbf{Y})}{2n} + \mathbf{o}\left(n^{-\frac{3}{2}}\right)\right], \tag{50}$$

where

$$v_0(\mathbf{Y}) = -\frac{\mathbf{Y}^2}{2} + \mathbf{Y}\mathbf{Z} - \frac{\mathbf{Z}^2}{2} \tag{51a}$$

$$v_1(\mathbf{Y}) = -\frac{\mathbf{Y}^3}{6} - \mathbf{Z}^2\mathbf{Y} + \frac{\mathbf{Z}\mathbf{Y}^2}{2} + \frac{2\mathrm{tr}(\mathbf{Z}^3)}{3} \tag{51b}$$

$$v_2(\mathbf{Y}) = \frac{p\mathrm{tr}(\mathbf{Y}^2)}{12} - \frac{\mathrm{tr}^2(\mathbf{Y})}{12} - \frac{\mathbf{Y}^4}{24} - \frac{\mathbf{Y}^2\mathbf{Z}^2}{2} + \frac{\mathbf{Y}^3\mathbf{Z}}{6} + \mathbf{Y}\mathbf{Z}^3 - \frac{3\mathrm{tr}(\mathbf{Z}^4)}{4} \tag{51c}$$

with

$$\mathbf{Z} \triangleq \sqrt{n}(\mathbf{\Sigma}' - \mathbf{I}_p). \tag{52}$$

Similar to our arguments in Section III, $C_T(T)$ is calculated as:

$$C_T(t) = c \int \exp\left(v_0(\mathbf{Y}) + (it)u_0(\mathbf{Y})\right) \times \Bigg[1 + \frac{1}{\sqrt{n}}\big(v_1(\mathbf{Y}) + (it)u_1(\mathbf{Y})\big) + \frac{1}{n}\Big\{v_2(\mathbf{Y}) + (it)u_2(\mathbf{Y}) + \frac{1}{2}\left(v_1(\mathbf{Y}) + (it)u_1(\mathbf{Y})\right)^2\Big\} + \mathbf{o}\left(n^{-\frac{3}{2}}\right)\Bigg] d\mathbf{Y}, \tag{53}$$

where the exponential term is

$$\begin{aligned}\exp\left(v_0(\mathbf{Y}) + (it)u_0(\mathbf{Y})\right) &= \mathrm{etr}\left((it)\mathbf{Z}^2\phi\right) \\ &\times \exp\left(-\frac{1}{2\phi}\left[\mathrm{tr}\left(\mathbf{Y} - \phi\mathbf{Z}\right)^2 + (2it)\phi\mathrm{tr}(\mathrm{Tr}(\mathbf{Y})^2)\right]\right).\end{aligned} \tag{54}$$

Since $\mathrm{Tr}(\mathbf{Z}) = \mathbf{0}_{m\times m}$, we have $\mathrm{Tr}(\mathbf{Y}) = \mathrm{Tr}(\mathbf{Y} - \mathbf{Z})$. Therefore, the p^2 variables of $\mathbf{Y}$ can be considered as Gaussian distributed with mean $\mathbb{E}\{\mathbf{Y}_{j,k}\} = \phi\mathbf{Z}_{j,k}$ and covariance matrix provided in (44). Consequently, $C_T(T)$ is expressed as:

$$C_T(t) = c_1\mathbb{E}\left[\left\{1 + \frac{1}{\sqrt{n}}\big(\mathbf{v}_1(\mathbf{Y}) + (it)u_1(\mathbf{Y})\big) + \frac{1}{n}\left\{v_2(\mathbf{Y}) + (it)u_2(\mathbf{Y}) + \frac{1}{2}\left(v_1(\mathbf{Y}) + (it)u_1(\mathbf{Y})\right)^2\right\} + \mathbf{o}\left(n^{-\frac{3}{2}}\right)\right\}\right]. \tag{55}$$

Furthermore, the moments involved in (55) are listed in Table III of Appendix E. Substituting these moments into (55) yields the following asymptotic result for the characteristic function:

$$C_T(t) = \phi^{\frac{f}{2}} \exp\left((it)a_2\phi\right)\left[\sum_{k=0}^{3} h_k\phi^k + \sum_{k=0}^{6} g_k\phi^k + \mathbf{o}\left(n^{-\frac{3}{2}}\right)\right], \tag{56}$$

where

$$g_0 = \frac{2a_3}{3\sqrt{n}} + \frac{e_2}{2qn} + \frac{2a_3^2}{9n} - \frac{3a_4}{4n} \tag{57a}$$

$$g_1 = -\frac{a_3}{\sqrt{n}} + \frac{b_2}{2qn} - \frac{3e_2}{2qn} + \frac{3a_4}{2n} - \frac{2a_3^2}{3n} \tag{57b}$$

$$g_2 = \frac{a_3^2}{2n} + \frac{e_2}{2qn} + \frac{a_2 p}{2n} \tag{57c}$$

$$g_3 = \frac{a_3}{3\sqrt{n}} + \frac{b_2}{2qn} + \frac{e_2}{qn} + \frac{a_2 m}{qn} - \frac{a_4}{n} - \frac{a_2 p}{n} + \frac{2a_3^2}{9n} \tag{57d}$$

$$g_4 = -\frac{a_3^2}{3n} - \frac{b_2}{qn} - \frac{a_2 m}{qn} - \frac{a_4}{4n} + \frac{pa_2}{2n} \tag{57e}$$

$$g_5 = \frac{a_4}{2n} - \frac{e_2}{2qn} \tag{57f}$$

$$g_6 = \frac{a_3^2}{18n} \tag{57g}$$

with $a_i = \text{tr}(\mathbf{Z}^i)$, $b_2 = \sum_{i,j=1}^{q} |\text{tr}(\mathbf{Z}_{ij})|^2$ and $e_2 = \text{tr}(\text{Tr}(\mathbf{Z}^2)^2)$. Inverting this characteristic function, we obtain (18). This ends the proof of Theorem 3. ∎

Appendix C
Proof of Theorem 5

For the high SNR case, we define:

$$\mathbf{X} \triangleq \frac{\mathbf{S} - n\boldsymbol{\Sigma}}{\sqrt{n}}. \tag{58}$$

Using (58), the asymptotic expansion of T under this setting is:

$$T = n\text{tr}\big(\mathbf{Z}'^2\big) + \sqrt{n}q_0(\mathbf{X}) + q_1(\mathbf{X}) + \mathbf{o}(n^{-\frac{1}{2}}) \tag{59}$$

where

$$q_0(\mathbf{X}) = \text{tr}\big(2\mathbf{Z}'\big(\mathbf{X} - \boldsymbol{\Sigma}\mathbf{I}_q \otimes \text{Tr}(\mathbf{X})/q\big)\big) \tag{60a}$$

$$q_1(\mathbf{X}) = \text{tr}\big(2\mathbf{Z}'\big(\boldsymbol{\Sigma}\mathbf{I}_q \otimes \text{Tr}(\mathbf{X})^2/q^2 - \mathbf{X}\mathbf{I}_q \otimes \text{Tr}(\mathbf{X})/q\big) + \big(\mathbf{X} - \boldsymbol{\Sigma}\mathbf{I}_q \otimes \text{Tr}(\mathbf{X})/q\big)^2\big). \tag{60b}$$

Clearly, the mean and variance of T can be respectively approximated as:

$$u = n\text{tr}(\mathbf{Z}'^2) + \sqrt{n}\mathbb{E}[q_0(\mathbf{X})] + \mathbb{E}[q_1(\mathbf{X})] + \mathbf{o}(n^{-\frac{1}{2}}) \tag{61a}$$

$$v = n\mathbb{E}[q_0^2(\mathbf{X})] + 2\sqrt{n}\mathbb{E}[q_0(\mathbf{X})q_1(\mathbf{X})] + \mathbf{o}(1). \tag{61b}$$

Expressing $q_0(\mathbf{X})$ and $q_1(\mathbf{X})$ in terms of $\mathbf{S}$, we have

$$q_0(\mathbf{X}) = \frac{1}{q\sqrt{n}}\text{tr}\big(2\mathbf{Z}'\big(q\mathbf{S} - \boldsymbol{\Sigma}\mathbf{I}_q \otimes \text{Tr}(\mathbf{S})\big)\big) \tag{62a}$$

$$q_1(\mathbf{X}) = \frac{1}{q^2 n}\text{tr}\big(\big(\mathbf{S} - \boldsymbol{\Sigma}\mathbf{I}_q \otimes \text{Tr}(\mathbf{S})\big)^2 + \boldsymbol{\Sigma}\mathbf{I}_q \otimes (\text{Tr}(\mathbf{S}) - nq\mathbf{I}_m)^2 - q(\mathbf{S} - n\boldsymbol{\Sigma})\mathbf{I}_q \otimes (\text{Tr}(\mathbf{S}) - nq\mathbf{I}_m)\big). \tag{62b}$$

Since $\text{Tr}(\boldsymbol{\Sigma}) = q\mathbf{I}_m$, it is straightforward to obtain

$$\mathbb{E}\left[q_0(\mathbf{X})\right] = \frac{1}{\sqrt{n}}\text{tr}\big(2\mathbf{Z}'(\boldsymbol{\Sigma} - \boldsymbol{\Sigma}\mathbf{I}_q \otimes \mathbf{I}_m)\big) = 0. \tag{63}$$

Moreover, using [33]

$$\mathbb{E}\left[\mathbf{S}_{r,s}\mathbf{S}_{k,l}\right] = (n^2\boldsymbol{\Sigma}_{r,s}\boldsymbol{\Sigma}_{k,l} + n\boldsymbol{\Sigma}_{k,s}\boldsymbol{\Sigma}_{r,l}), \tag{64}$$

we have

$$\begin{aligned}\mathbb{E}\left[q_1(\mathbf{X})\right] &= \text{tr}(\boldsymbol{\Sigma})^2 - \frac{2}{q}\sum_{i,j=1}^{q}\text{tr}(\boldsymbol{\Sigma}_{ij})\text{tr}((\boldsymbol{\Sigma}^2)_{ji}) + \frac{1}{q^2}\sum_{i,j,k,l=1}^{q}|\text{tr}(\boldsymbol{\Sigma}_{ij}\boldsymbol{\Sigma}_{kl})|^2 \\ &\quad + \frac{2}{q^2}\sum_{i,j,k=1}^{q}\text{tr}(\boldsymbol{\Sigma}_{ij})\text{tr}((\mathbf{Z}\boldsymbol{\Sigma})_{kk}\boldsymbol{\Sigma}_{ji}) - \frac{2}{q}\sum_{i,j=1}^{q}\text{tr}((\mathbf{Z}\boldsymbol{\Sigma})_{ij})\text{tr}(\boldsymbol{\Sigma}_{ji})\end{aligned} \tag{65}$$

and

$$\mathbb{E}\left[q_0^2(\mathbf{X})\right] = 4\text{tr}\big((\mathbf{Z}\boldsymbol{\Sigma})^2\big) - \frac{8}{q}\text{tr}\big(\text{Tr}(\boldsymbol{\Sigma}\mathbf{Z}\boldsymbol{\Sigma})\text{Tr}(\mathbf{Z}\boldsymbol{\Sigma})\big) + \frac{4}{q^2}\text{tr}\big(\text{Tr}(\mathbf{Z}\boldsymbol{\Sigma})\text{Tr}(\boldsymbol{\Sigma}(\mathbf{I}_q \otimes \text{Tr}(\mathbf{Z}\boldsymbol{\Sigma}))\boldsymbol{\Sigma})\big). \tag{66}$$

On the other hand, using the central limit theorem, we conclude that $\mathbf{W} = \boldsymbol{\Sigma}^{-\frac{1}{2}}\mathbf{X}\boldsymbol{\Sigma}^{-\frac{1}{2}}$ has an approximate probability distribution function as

$$f(\mathbf{W}) = c_3 \times \exp\left(-\frac{1}{2}\text{tr}(\mathbf{W}^2)\right) + \mathbf{o}\left(n^{-\frac{1}{2}}\right), \tag{67}$$

which signifies that each element of $\mathbf{W}$ asymptotically obeys zero mean Gaussian distribution, suggesting that the dominant term of the third moments of $\mathbf{X}$ embedded in (61) equal zero, namely,

$$\mathbb{E}[q_0(\mathbf{X})q_1(\mathbf{X})] = 0 + \mathbf{o}\left(n^{-\frac{1}{2}}\right). \tag{68}$$

Substituting (63), (65)-(66) and (68) into (61) results in (22). This ends the proof of Theorem 5.

Appendix D
Proof of (36)

Proof: Recalling that $\mathbf{Y}$ is defined as $\mathbf{Y} = \sqrt{n}\log(\mathbf{S}/n)$, it is easy to obtain

$$\frac{1}{n}\mathbf{S} = \mathbf{I}_p + \frac{\mathbf{Y}}{\sqrt{n}} + \frac{\mathbf{Y}^2}{2n} + \frac{\mathbf{Y}^3}{6\sqrt{n}^3} + \frac{\mathbf{Y}^4}{24n^2} + \mathcal{O}\left(n^{-\frac{5}{2}}\right). \tag{69}$$

To expand $(\mathbf{I}_q \otimes \text{Tr}(\mathbf{S}))^{-1}$, the following lemma regarding matrix inverse is needed [35, pp. 55].

Lemma 1: Let $\mathbf{A} \in \mathbb{C}^{p\times p}$ and $\lim_{k\to\infty}\mathbf{A}^k = \mathbf{0}_{p\times p}$. Then $\mathbf{I}_p - \mathbf{A}$ is nonsingular and

$$(\mathbf{I}_p - \mathbf{A})^{-1} = \sum_{k=0}^{\infty}\mathbf{A}^k. \tag{70}$$

By setting

$$\mathbf{A} = -\frac{\mathbf{I}_q}{q} \otimes \text{Tr}\left[\frac{\mathbf{Y}}{\sqrt{n}} + \frac{\mathbf{Y}^2}{2n} + \frac{\mathbf{Y}^3}{6\sqrt{n}^3} + \frac{\mathbf{Y}^4}{24n^2}\right] \tag{71}$$

and applying Lemma 1, we can express $(\mathbf{I}_q \otimes \text{Tr}(\mathbf{S}))^{-1}$ as

$$\begin{aligned}\left(\frac{(\mathbf{I}_q \otimes \text{Tr}(\mathbf{S}))}{qn}\right)^{-1} &= \mathbf{I}_p - \frac{1}{\sqrt{n}}\mathbf{I}_q \otimes \frac{\text{Tr}(\mathbf{Y})}{q} + \frac{1}{n}\mathbf{I}_q \otimes \left[\frac{\text{Tr}^2(\mathbf{Y})}{q^2} - \frac{\text{Tr}(\mathbf{Y}^2)}{2q}\right] \\ &\quad + \frac{1}{\sqrt{n}^3}\mathbf{I}_q \otimes \left[\frac{\text{Tr}(\mathbf{Y})\text{Tr}(\mathbf{Y}^2)}{q^2} + \frac{\text{Tr}(\mathbf{Y}^2)\text{Tr}(\mathbf{Y})}{q^2} - \frac{\text{Tr}(\mathbf{Y}^3)}{6q}\right.\end{aligned}$$

TABLE II
MOMENTS INVOLVED IN (46)

	Expectation
$\mathrm{tr}^2(\mathbf{Y})$	p
$\mathrm{tr}(\mathbf{Y}^2)$	$(p^2-m^2)\phi+m^2$
$\mathrm{tr}(\mathrm{Tr}(\mathbf{Y})^4)$	$mq^2(2m^2+1)$
$\mathrm{tr}(\mathrm{Tr}^2(\mathbf{Y})\mathrm{Tr}(\mathbf{Y}^2))$	$(p^3-pm^2)\phi+p(2m^2+1)$
$\mathrm{tr}(\mathrm{Tr}^2(\mathbf{Y}^2))$	$(m^3q^4-m^3q^2+mq^2-m)\phi^2-(2m^3-2m^3q^2)\phi+2m^3+m$
$\mathrm{tr}(\mathrm{Tr}(\mathbf{Y})\mathrm{Tr}(\mathbf{Y}^3))$	$m(q^2-1)(2m^2+1)\phi+m(2m^2+1)$
$\mathrm{tr}((\mathbf{Y}\otimes(\mathbf{I}_q,\mathrm{Tr}(\mathbf{Y})))^2)$	$p(q^2-1)\phi+p(2m^2+1)$
$\mathrm{tr}(\mathrm{Tr}(\mathbf{Y})\mathrm{Tr}(\mathbf{Y}^2))^2$	$(p^3q^2-p^3+pq^2-p)\phi^2-p(6m^2-6m^2q^2)\phi+p(12m^2+3)$
$\mathrm{tr}^2(\mathrm{Tr}^3(\mathbf{Y}))$	$12p^3+3pq^2$
$\mathrm{tr}(\mathbf{Y}^3)^2$	$(-6p-9m^3q+3p^3+\frac{6m^3+6m}{q})\phi^3+(9p-9m^2p+9p^3-\frac{9m}{q})\phi^2+(18m^2p-\frac{18m^3}{q})\phi+\frac{12m^3+3m}{q}$
$\mathrm{tr}(\mathrm{Tr}(\mathbf{Y})\mathrm{Tr}(\mathbf{Y}^2))\mathrm{tr}(\mathrm{Tr}^3(\mathbf{Y}))$	$(3p^3q-mp^2)\phi+12mp^2+3pq$
$\mathrm{tr}(\mathrm{Tr}(\mathbf{Y})\mathrm{Tr}(\mathbf{Y}^2))\mathrm{tr}(\mathbf{Y}^3)$	$(3p^3q-3mp^2+3pq-3m)\phi^2-(12m^3-12mp^2)\phi+3m(4m^2+1)$
$\mathrm{tr}(\mathrm{Tr}^3(\mathbf{Y}))\mathrm{tr}(\mathbf{Y}^3)$	$(9p^3-9pm^2)\phi+3p(4m^2+1)$

$$+\frac{\mathrm{Tr}^3(\mathbf{Y})}{q^3}\Bigg]+\frac{1}{n^2}\mathbf{I}_q\otimes\Bigg[\frac{\mathrm{Tr}^2(\mathbf{Y}^2)}{q^2}-\frac{\mathrm{Tr}(\mathbf{Y}^4)}{6q}-\frac{\mathrm{Tr}^4(\mathbf{Y})}{q^4}$$
$$+\frac{2\mathrm{Tr}(\mathbf{Y})\mathrm{Tr}(\mathbf{Y}^3)}{3q^2}+\frac{2\mathrm{Tr}(\mathbf{Y}^3)\mathrm{Tr}(\mathbf{Y})}{3q^2}-\frac{2\mathrm{Tr}^2(\mathbf{Y})\mathrm{Tr}(\mathbf{Y}^2)}{q^3}$$
$$-\frac{2\mathrm{Tr}(\mathbf{Y})\mathrm{Tr}(\mathbf{Y}^2)\mathrm{Tr}(\mathbf{Y})}{q^3}-\frac{2\mathrm{Tr}(\mathbf{Y}^2)\mathrm{Tr}^2(\mathbf{Y})}{q^3}\Bigg]+\mathcal{O}\left(n^{-\frac{5}{2}}\right). \tag{72}$$

Substituting (69) and (72) into (10) leads to the asymptotic series expansion of T:

$$T=\mathrm{tr}(\mathbf{Y}^2)-\frac{1}{q}\mathrm{tr}(\mathrm{Tr}(\mathbf{Y})^2)+\frac{1}{\sqrt{n}}\Bigg[\mathrm{tr}(\mathrm{Tr}(\mathbf{Y}^3))+\frac{2}{q^2}\mathrm{tr}(\mathrm{Tr}(\mathbf{Y})^3)$$
$$-\frac{3}{q}\mathrm{tr}(\mathrm{Tr}(\mathbf{Y})\mathrm{Tr}(\mathbf{Y}^2))\Bigg]+\frac{1}{n}\Bigg[\frac{7}{12}\mathrm{tr}(\mathbf{Y}^4)-\frac{3}{q^3}\mathrm{tr}(\mathrm{Tr}(\mathbf{Y})^4)$$
$$-\frac{7}{3q}\mathrm{tr}(\mathrm{Tr}(\mathbf{Y})\mathrm{Tr}(\mathbf{Y}^3))+\frac{1}{q^2}\mathrm{tr}((\mathbf{Y}(\mathbf{I}_q\otimes\mathrm{Tr}(\mathbf{Y})))^2)$$
$$+\frac{5}{q^2}\mathrm{tr}(\mathrm{Tr}(\mathbf{Y})^2\mathrm{Tr}(\mathbf{Y}^2))-\frac{5}{4q}\mathrm{tr}(\mathrm{Tr}(\mathbf{Y}^2)^2)\Bigg]+\mathbf{o}\left(n^{-\frac{3}{2}}\right). \tag{73}$$

■

APPENDIX E
DERIVATION OF MOMENTS IN (46) AND (55)

In order to simplify the moment computations, we need to resort to the following results.

Lemma 2: Let $\mathbf{A}$ be a $p\times p$ Hermitian random matrix whose p^2 free parameters are mutually independent zero mean Gaussian variables with variances:

$$\mathbb{V}(\mathbf{A}_{j,j})=1 \qquad j=1,\cdots,p \tag{74a}$$
$$\mathbb{V}(\mathbf{A}^R_{j,k})=\tfrac{1}{2} \qquad j,k=1,\cdots,p,\ j<k \tag{74b}$$
$$\mathbb{V}(\mathbf{A}^I_{j,k})=\tfrac{1}{2} \qquad j,k=1,\cdots,p,\ j<k. \tag{74c}$$

Using the subscript pairs $(i,j)=a$, $(k,1)=b$, $(m,n)=c$, $(q,r)=d$, $(s,t)=e$ and $(u,v)=f$, we have:

$$\mathbb{E}[\mathbf{A}_a\mathbf{A}_b\mathbf{A}_c\mathbf{A}_d]=\delta(a,b)\delta(c,d)$$
$$+\delta(a,c)\delta(b,d)+\delta(a,d)\delta(b,c) \tag{75a}$$
$$\mathbb{E}[\mathbf{A}_a\mathbf{A}_b\mathbf{A}_c\mathbf{A}_d\mathbf{A}_e\mathbf{A}_f]=$$
$$\delta(a;b)[\delta(c;d)\delta(e;f)+\delta(c;e)\delta(d;f)+\delta(c;f)\delta(d;e)]$$
$$+\delta(a;c)[\delta(b;d)\delta(e;f)+\delta(b;e)\delta(d;f)+\delta(b;f)\delta(d;e)]$$
$$+\delta(a;d)[\delta(b;c)\delta(e;f)+\delta(b;e)\delta(c;f)+\delta(b;f)\delta(c;e)]$$
$$+\delta(a;e)[\delta(b;c)\delta(d;f)+\delta(b;d)\delta(c;f)+\delta(b;f)\delta(c;d)]$$
$$+\delta(a;f)[\delta(b;c)\delta(d;e)+\delta(b;d)\delta(c;e)+\delta(b;e)\delta(c;d)], \tag{75b}$$

where $\delta(i,j;k,l)$ equals 1 if $i=l,k=j$, and 0 otherwise.

The proof of Lemma 2 is provided as follows. Based on (74), we have

$$\mathbb{E}[\mathbf{A}_{i,j}\mathbf{A}_{k,l}]=\delta(i,j;k,l) \tag{76a}$$
$$\mathbb{E}[\mathbf{A}^2_{i,j}\mathbf{A}^2_{j,i}]=\begin{cases}2 & i\neq j\\ 3 & i=j\end{cases} \tag{76b}$$
$$\mathbb{E}[\mathbf{A}^3_{i,j}\mathbf{A}^3_{j,i}]=\begin{cases}6 & i\neq j\\ 15 & i=j\end{cases}. \tag{76c}$$

Recall that the odd moments of $\mathbf{A}$ equal zero, which, when combined with (76) leads to (75). This completes the proof of Lemma 2.

However, Lemma 2 cannot be directly applied to (46) since some elements of $\mathbf{Y}$ are correlated. Therefore, we need to define two independent Hermitian matrices $\mathbf{X}\in\mathbb{R}^{p\times p}$ and $\mathbf{W}\in\mathbb{R}^{m\times m}$, which are in form of $\mathbf{A}$ in Lemma 2. Consequently, $\mathbf{Y}$ can be expressed as

$$\mathbf{Y}=\phi^{\frac{1}{2}}\mathbf{X}+\sigma^{\frac{1}{2}}\mathbf{I}_q\otimes\mathbf{W}. \tag{77}$$

TABLE III
MOMENTS INVOLVED IN (46)

	Expectation
$\mathrm{tr}^2(\mathbf{Y})$	p
$\mathrm{tr}(\mathbf{Y}^2)$	$(p^2-m^2)\phi+m^2$
$\mathrm{tr}(\mathrm{Tr}(\mathbf{Y})^4)$	$mq^2(2m^2+1)$
$\mathrm{tr}(\mathbf{Y}^2\mathbf{Z}^2)$	$a_4\phi^4+(a_2mq-\frac{a_2m}{q})\phi^3+\frac{a_2m}{q}\phi^2$
$\mathrm{tr}(\mathbf{Y}^3\mathbf{Z})$	$a_4\phi^4+(2a_2mq-\frac{b_2+2a_2m}{q})\phi^3+\frac{b_2+2a_2m}{q}\phi^2$
$\mathrm{tr}(\mathrm{Tr}^2(\mathbf{Y})\mathrm{Tr}(\mathbf{Y}^2))$	$a_2p\phi^2+(p^3-pm^2)\phi+p(2m^2+1)$
$\mathrm{tr}(\mathrm{Tr}^2(\mathbf{Y}^2))$	$(2a_2mq^2+2b_2)\phi^3+(e_2+2a_2m)\phi^2+(m^3q^4-m^3q^2+mq^2-m)\phi^2-(2m^3-2m^3q^2)\phi+2m^3+m$
$\mathrm{tr}(\mathrm{Tr}(\mathbf{Y})\mathrm{Tr}(\mathbf{Y}^3))$	$(b_2+2a_2m)\phi^2+m(q^2-1)(2m^2+1)\phi+m(2m^2+1)$
$\mathrm{tr}((\mathbf{Y}\otimes(\mathbf{I}_q,\mathrm{Tr}(\mathbf{Y})))^2)$	$b_2q\phi^2+p(q^2-1)\phi+p(2m^2+1)$
$\mathrm{tr}(\mathrm{Tr}(\mathbf{Y})\mathrm{Tr}(\mathbf{Y}^2))^2$	$q(2a_2mq^2+2b_2)\phi^3+q(g2+6a_2m)\phi^2+(p^3q^2-p^3+pq^2-p)\phi^2-p(6m^2-6m^2q^2)\phi+p(12m^2+3)$
$\mathrm{tr}^2(\mathrm{Tr}^3(\mathbf{Y}))$	$12p^3+3pq^2$
$\mathrm{tr}(\mathbf{Y}^3)^2$	$a_3^2\phi^6+9a_4\phi^5+(9a_2p-\frac{18b_2+18a_2m}{q})\phi^4+(\frac{18b_2-9e_2}{q}+18a_2p)\phi^3+\frac{9e_2+18a_2m}{q}\phi^2$
	$+(-6p-9m^3q+3p^3+\frac{6m^3+6m}{q})\phi^3+(9p-9m^2p+9p^3-\frac{9m}{q})\phi^2+(18m^2p-\frac{18m^3}{q})\phi+\frac{12m^3+3m}{q}$
$\mathrm{tr}(\mathrm{Tr}(\mathbf{Y})\mathrm{Tr}(\mathbf{Y}^2))\mathrm{tr}(\mathrm{Tr}^3(\mathbf{Y}))$	$(3a_2pq)\phi^2+(3p^3q-mp^2)\phi+12mp^2+3pq$
$\mathrm{tr}(\mathrm{Tr}(\mathbf{Y})\mathrm{Tr}(\mathbf{Y}^2))\mathrm{tr}(\mathbf{Y}^3)$	$(6a_2mq^2+6b_2)\phi^3+12a_2m\phi^2+3e_2+(3p^3q-3mp^2+3pq-3m)\phi^2-(12m^3-12mp^2)\phi+3m(4m^2+1)$
$\mathrm{tr}(\mathrm{Tr}^3(\mathbf{Y}))\mathrm{tr}(\mathbf{Y}^3)$	$(9a_2p)\phi^2+(9p^3-9pm^2)\phi+3p(4m^2+1)$
$\mathrm{tr}(\mathbf{Y}\mathbf{Z}^2)^2$	$a_3^2\phi^6+a_4\phi^5-\frac{e_2\phi^3}{q}+\frac{e_2\phi^2}{q}$
$\mathrm{tr}(\mathbf{Y}^2\mathbf{Z})^2$	$a_3^2\phi^6+4a_4\phi^5+(a_2p-\frac{2b_2}{q}-\frac{2a_2m}{q})\phi^4+(\frac{2b_2}{q}-\frac{4e_2}{q}+\frac{2a_2m}{q})\phi^3+\frac{4e_2}{q}\phi^2$
$\mathrm{tr}(\mathbf{Y}^2\mathbf{Z})\mathrm{tr}(\mathbf{Y}\mathbf{Z}^2)$	$a_3^2\phi^6+2a_4\phi^5-\frac{2e_2\phi^3}{q}+\frac{2e_2\phi^2}{q}$
$\mathrm{tr}(\mathbf{Y}\mathbf{Z}^2)\mathrm{tr}(\mathbf{Y}^3)$	$a_3^2\phi^6+3a_4\phi^5+(3a_2mq-\frac{3e_2+3a_2m}{q})\phi^3+\frac{3e_2+3a_2m}{q}\phi^2$
$\mathrm{tr}(\mathbf{Y}\mathbf{Z}^2)\mathrm{tr}(\mathbf{Y}^3)$	$a_3^2\phi^6+6a_4\phi^5+(3a_2p-\frac{6b_2+6a_2m}{q})\phi^4+(\frac{6b_2-6e_2}{q}+6a_2p)\phi^3+\frac{6e_2+6a_2m}{q}\phi^2$
$\mathrm{tr}(\mathbf{Y}\mathbf{Z}^2)\mathrm{tr}(\mathrm{Tr}(\mathbf{Y})\mathrm{Tr}(\mathbf{Y}^2))$	$(a_2mq^2-a_2m)\phi^3+(e_2+3a_2m)\phi^2$
$\mathrm{tr}(\mathbf{Y}^2\mathbf{Z})\mathrm{tr}(\mathrm{Tr}(\mathbf{Y})\mathrm{Tr}(\mathbf{Y}^2))$	$(2a_2mq^2+2b_2)\phi^3+(2e_2+6a_2m)\phi^2$
$\mathrm{tr}(\mathbf{Y}\mathbf{Z}^2)\mathrm{tr}(\mathrm{Tr}^3(\mathbf{Y}))$	$(3a_2p)\phi^2$
$\mathrm{tr}(\mathbf{Y}^2\mathbf{Z})\mathrm{tr}(\mathrm{Tr}^3(\mathbf{Y}))$	$(6a_2p)\phi^2$

As a result, we have

$$\mathbb{E}[\mathrm{tr}(\mathbf{Y}^4)]=\phi^2\mathbb{E}[\mathrm{tr}(\mathbf{X}^4)]+4\phi\sigma\mathbb{E}[\mathrm{tr}(\mathbf{X}^2(\mathbf{I}\otimes\mathbf{W})^2)]+2\phi\sigma\mathbb{E}[\mathrm{tr}((\mathbf{X}(\mathbf{I}\otimes\mathbf{W}))^2)]+q\sigma^2\mathbb{E}[\mathrm{tr}(\mathbf{W}^4)]. \tag{78}$$

Moreover, applying Lemma 2, the expectations on the right hand side (r.h.s.) are calculated as

$$\mathbb{E}[\mathrm{tr}(\mathbf{X}^4)]=\mathbb{E}\left[\sum_{i,j,k,l=1}^{p}\mathbf{Y}_{i,j}\mathbf{Y}_{j,k}\mathbf{Y}_{k,l}\mathbf{Y}_{l,i}\right]=2p^3+p \tag{79a}$$

$$\mathbb{E}[\mathrm{tr}(\mathbf{X}^2(\mathbf{I}_q\otimes\mathbf{W})^2)]=\sum_{r,s=1}^{q}\mathbb{E}\left[\sum_{i,j,k,l=1}^{m}(\mathbf{X}_{rs})_{i,j}(\mathbf{X}_{sr})_{j,k}\mathbf{W}_{k,l}\mathbf{W}_{l,i}\right]=q^2m^3 \tag{79b}$$

$$\mathbb{E}[\mathrm{tr}((\mathbf{X}(\mathbf{I}_q\otimes\mathbf{W}))^2)]=\sum_{r,s=1}^{q}\mathbb{E}\left[\sum_{i,j,k,l=1}^{m}(\mathbf{X}_{rs})_{i,j}\mathbf{W}_{j,k}(\mathbf{X}_{sr})_{k,l}\mathbf{W}_{l,i}\right]=q^2m \tag{79c}$$

$$\mathbb{E}[\mathrm{tr}(\mathbf{W}^4)]=\mathbb{E}\left[\sum_{i,j,k,l=1}^{p}\mathbf{W}_{i,j}\mathbf{W}_{j,k}\mathbf{W}_{k,l}\mathbf{W}_{l,i}\right]=2m^3+m. \tag{79d}$$

Noticing that $\sigma=(1-\phi)/q$, we eventually have

$$\mathbb{E}[\mathrm{tr}(\mathbf{Y}^4)]=\left(2p^3-4m^3q-mq+\frac{2m^3+m}{q}\right)\phi^2+\left(4m^3q+2p-\frac{4m^3+2m}{q}\right)\phi+\frac{2m^3+m}{q}. \tag{80}$$

Similarly, the other moments in (46) can also be determined accordingly, which are tabulated in Table II.

In (55), the expectation of $\mathbf{Y}$ is changed to $\phi\mathbf{Z}$, which enables us to modify (77) as

$$\mathbf{Y}=\phi\mathbf{Z}+\phi^{\frac{1}{2}}\mathbf{X}+\sigma^{\frac{1}{2}}\mathbf{I}_q\otimes\mathbf{W}. \tag{81}$$

Here we take $\mathrm{tr}(\mathbf{Y}^4)$ as an example, with the remaining terms listed in Table III. Based on (81), we have

$$\mathbb{E}[\mathrm{tr}(\mathbf{Y}^4)]=\mathbb{E}[\mathrm{tr}((\phi^{\frac{1}{2}}\mathbf{X}+\sigma^{\frac{1}{2}}\mathbf{I}\otimes\mathbf{W})^4)]+4\phi^3\mathbb{E}[\mathrm{tr}(\mathbf{X}^2\mathbf{Z}^2)]+2\phi^3\mathbb{E}[\mathrm{tr}((\mathbf{X}\mathbf{Z})^2)]+2\phi^2\sigma\mathbb{E}[\mathrm{tr}(((\mathbf{I}\otimes\mathbf{W})\mathbf{Z})^2)]+4\phi^2\sigma\mathbb{E}[\mathrm{tr}((\mathbf{I}\otimes\mathbf{W})^2\mathbf{Z}^2)]+\phi^4\mathrm{tr}(\mathbf{Z}^4). \tag{82}$$

Using Lemma 2, the expectations in the r.h.s. of (82) are calculated as

$$\mathbb{E}[\mathrm{tr}(\mathbf{X}^2\mathbf{Z}^2)] = \sum_{r,s=1}^{q} \mathbb{E}\left[\sum_{i,j,k,l=1}^{m} \mathbf{X}_{i,j}\mathbf{X}_{j,k}\mathbf{Z}_{k,l}\mathbf{Z}_{l,i}\right] = p\phi a_2 \quad (83a)$$

$$\mathbb{E}[\mathrm{tr}((\mathbf{XZ})^2)] = \sum_{r,s=1}^{q} \mathbb{E}\left[\sum_{i,j,k,l=1}^{m} \mathbf{X}_{i,j}\mathbf{Z}_{j,k}\mathbf{X}_{k,l}\mathbf{Z}_{l,i}\right] = \mathrm{tr}^2(\mathbf{Z}) = 0 \quad (83b)$$

$$\mathbb{E}[\mathrm{tr}((\mathbf{I}_q \otimes \mathbf{W})^2\mathbf{Z}^2)] = \sum_{r,s=1}^{q} \mathbb{E}\left[\mathbf{W}_{i,j}\mathbf{W}_{j,k}(\mathbf{Z}_{rs}\mathbf{Z}_{sr})_{k,i}\right] = ma_2 \quad (83c)$$

$$\mathbb{E}[\mathrm{tr}(((\mathbf{I}_q \otimes \mathbf{W})\mathbf{Z})^2)] = \sum_{r,s=1}^{q} \mathbb{E}\left[\mathbf{W}_{i,j}(\mathbf{Z}_{rs})_{j,k}\mathbf{W}_{k,l}(\mathbf{Z}_{sr})_{l,i}\right] = b_2. \quad (83d)$$

Substituting (83) and (80) into (82) yields

$$\begin{aligned}\mathbb{E}[\mathrm{tr}(\mathbf{Y}^4)] &= (2p^3 - 4m^3q - mq + \frac{2m^3+m}{q})\phi^2 \\ &+ \left(4m^3q + 2p - \frac{4m^3+2m}{q}\right)\phi + \frac{2m^3+m}{q} \\ &+ a_4\phi^4 + \left(4a_2mq - \frac{2b_2+4a_2m}{q}\right)\phi^3 \\ &+ \frac{2b_2+4a_2m}{q}\phi^2. \end{aligned} \quad (84)$$

ACKNOWLEDGMENT

The authors would like to thank the anonymous reviewers for their constructive comments which significantly improved this paper.

REFERENCES

[1] D. Ramírez, J. Vía, I. Santamaría, and L. L. Scharf, "Locally most powerful invariant tests for correlation and sphericity of Gaussian vectors," *IEEE Trans. Inf. Theory*, vol. 59, no. 4, pp. 2128–2141, Apr. 2013.
[2] D. B. Williams and D. H. Johnson, "Using the sphericity test for source detection with narrow-band passive arrays," *IEEE Trans. Acoust., Speech, Signal Process.*, vol. 38, no. 11, pp. 2008–2014, Nov. 1990.
[3] J. Li and P. Stoica, *MIMO Radar Signal Processing*. New York, NY, USA: Wiley, 2008.
[4] Y. Abramovich, N. Spencer, and A. Gorokhov, "Detection-estimation of more uncorrelated Gaussian sources than sensors in nonuniform linear antenna arrays: Part I: Fully augmentable arrays," *IEEE Trans. Image Process.*, vol. 49, no. 5, pp. 959–971, May 2001.
[5] R. Kakarala and P. O. Ogunbona, "Signal analysis using a multiresolution form of the singular value decomposition," *IEEE Trans. Image Process.*, vol. 10, no. 5, pp. 724–735, May 2001.
[6] L. Huang, J. Fang, K. Liu, H. C. So, and H. Li, "An eigenvalue-moment-ratio approach to blind spectrum sensing for cognitive radio under sample-starving environment," *IEEE Trans. Veh. Technol.*, vol. 64, no. 8, pp. 3465–3480, Aug. 2015.
[7] L. Wei and O. Tirkkonen, "Spectrum sensing in the presence of multiple primary users," *IEEE Trans. Commun.*, vol. 60, no. 5, pp. 1268–1277, May 2012.
[8] L. Wei, P. Dharmawansa, and O. Tirkkonen, "Multiple primary user spectrum sensing in the low SNR regime," *IEEE Trans. Commun.*, vol. 16, no. 5, pp. 1720–1731, May 2013.
[9] J. Mauchly, "Significance test for sphericity of a normal n-variate distribution," *Ann. Statist*, vol. 11, no. 2, pp. 204–209, Jun. 1940.
[10] S. John, "Some optimal multivariate tests," *Biometrika*, vol. 58, no. 1, pp. 123–127, Apr. 1971.
[11] H. Nagao, "On some test criteria for covariance matrix," *Ann. Statist*, vol. 1, no. 4, pp. 700–709, Jul. 1973.
[12] E. Conte, A. De Maio, and G. Ricci, "Recursive estimation of the covariance matrix of a compound-Gaussian process and its application to adaptive CFAR detection," *IEEE Trans. Signal Process.*, vol. 50, no. 8, pp. 1908–1915, Aug. 2002.
[13] C. Y. Chong, F. Pascal, J. P. Ovarlez, and M. Lesturgie, "MIMO radar detection in non-Gaussian and heterogeneous clutter," *IEEE J. Sel. Topics Signal Process.*, vol. 4, no. 1, pp. 115–126, Feb. 2010.
[14] M. Akcakaya and A. Nehorai, "MIMO radar detection and adaptive design in compound-Gaussian clutter," in *Proc. IEEE Radar Conf.*, May 2010, pp. 236–241.
[15] E. J. Kelly, "An adaptive detection algorithm," *IEEE Trans. Aerosp. Electron. Syst.*, vol. AES-22, no. 2, pp. 115–127, Mar. 1986.
[16] Q. He, N. H. Lehmann, R. S. Blum, and A. M. Haimovich, "MIMO radar moving target detection in homogeneous clutter," *IEEE Trans. Aerosp. Electron. Syst.*, vol. 46, no. 3, pp. 1290–1301, Jul. 2010.
[17] L. Wei, O. Tirkkonen, and Y. C. Liang, "Multi-source signal detection with arbitrary noise covariance," *IEEE Trans. Signal Process.*, vol. 62, no. 2, pp. 5907–5918, Nov. 2014.
[18] M. I. Skolnik, *Introduction to Radar Systems*. New York, NY, USA: McGraw-Hill, 2001.
[19] A. Kisliansky, R. Shavit, and J. Tabrikian, "Direction of arrival estimation in the presence of noise coupling in antenna arrays," *IEEE Trans. Antennas Propag.*, vol. 55, no. 7, pp. 1940–1947, Jul. 2007.
[20] S. M. Kay, *Fundamentals of Statistical Signal Processing: Detection Theory*, vol. II. New York, NY, USA: Prentice-Hall, 1998.
[21] N. Sugiura, "Asymptotic non-null distributions of the likelihood ratio criteria for covariance matrix under local alternatives," *Ann. Statist.*, vol. 1, no. 4, pp. 718–728, Jul. 1973.
[22] H. Nagao, "Asymptotic nonnull distributions of certain test criteria for a covariance matrix," *J. Multivariate Anal.*, vol. 4, no. 4, pp. 409-418, Dec. 1974.
[23] H. Jiang, J. K. Zhang, and K. M. Wong, "Joint DOD and DOA estimation for bistatic MIMO radar in unknown correlated noise," *IEEE Trans. Veh. Technol.*, vol. 64, no. 11, pp. 5113–5125, Nov. 2015.
[24] L. Xu, J. Li, and P. Stoica, "Target detection and parameter estimation for MIMO radar systems," *IEEE Trans. Aerosp. Electron. Syst.*, vol. 44, no. 3, pp. 927–939, Jul. 2008.
[25] M. Jin, G. Liao, and J. Li, "Joint DOD and DOA estimation for bistatic MIMO radar," *Signal Process.*, vol. 89, no, 2, pp. 244–251, 2009.
[26] Y. Xiao, L. Huang, J. Xie, and H. C. So, "Approximate asymptotic distribution of locally most powerful invariant test for independence: Complex case," *IEEE Trans. Inf. Theory*, vol. 64, no. 3, pp. 1784–1799, Mar. 2018.
[27] Y. Xiao, L. Huang, J. Xie, and H. C. So, "Accurate asymptotic analysis for John's test in multichannel signal detection," in *Proc. IEEE Int. Conf. Acoust., Speech, Signal Process.*, Shanghai, China, Mar. 2016, pp. 4358–4362.
[28] G. E. P. Box, "A general distribution theory for a class of likelihood criteria," *Biometrika*, vol. 36, pp. 317–346, Dec. 1949.
[29] P. Ginzberg and A. T. Walden, "Testing for quaternion propriety," *IEEE Trans. Signal Process.*, vol. 59, no. 7, pp. 3025–3034, Jul. 2011.
[30] A. Mariani, A. Giorgetti, and M. Chiani, "Test of independence for cooperative spectrum sensing with uncalibrated receivers," in *Proc. IEEE GLOBECOM*, Anaheim, CA, USA, pp. 1374–1379, Dec. 2012.
[31] S. Sedighi, A. Taherpour, J. Sala, and T. Khattab, "On the performance of Hadamard ratio detector-based spectrum sensing for cognitive radios, *IEEE Trans. Signal Process.*, vol. 63, no. 14, pp. 3809–3824, Jul. 2015.
[32] T. W. Anderson, "On the distribution of the two-sample Cramér-von Mises criterion," *Ann. Math. Statist.*, vol. 33, no. 3, pp. 1148–1159, Sep. 1962.
[33] D. Maiwald and D. Kraus, "On moments of complex Wishart and complex inverse Wishart distributed matrices," in *Proc. IEEE Int. Conf. Acoust., Speech, Signal Process.*, Munich, Germany, Apr. 1997, pp. 3817–3820.

[34] S. S. Wilks, “Certain generalizations in the analysis of variance” *Biometrika*, vol. 24, no. 3/4, pp. 471–494, 1932.
[35] G. Stewart, *Matrix Algorithms: Volume 1, Basic Decompositions*, vol. 1. Cambridge, U.K.: Cambridge Univ. Press, 1998.

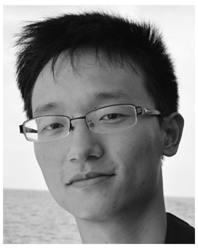

Yu-Hang Xiao was born on January 20, 1992, in Anhui, China. He received the B.E. degree in microelectronics from the Harbin Engineering University, Harbin, China, and the M.E. degree in information and communication engineering from the Harbin Institute of Technology (HIT), Harbin, China, in 2012 and 2014, respectively. Since September 2014, he has been working toward the Ph.D. degree in the field of information and communication engineering at HIT. During October 2015–February 2017, he was a visiting Ph.D. student with the Department of Electrical and Computer Engineering, McMaster University, Hamilton, ON, Canada. His research interests include statistical signal processing and MIMO communications.

Lei Huang (M’07–SM’14) was born in Guangdong, China. He received the B.Sc., M.Sc., and Ph.D. degrees in electronic engineering from Xidian University, Xian, China, in 2000, 2003, and 2005, respectively.

From 2005 to 2006, he was a Research Associate with the Department of Electrical and Computer Engineering, Duke University, Durham, NC, USA. From 2009 to 2010, he was a Research Fellow with the Department of Electronic Engineering, City University of Hong Kong, and a Research Associate with the Department of Electronic Engineering, The Chinese University of Hong Kong. From 2011 to 2014, he was a Professor with the Department of Electronic and Information Engineering, Harbin Institute of Technology Shenzhen Graduate School. Since November 2014, he has joined the College of Information Engineering, Shenzhen University, where he is currently a Distinguished Professor. His research interests include array signal processing, statistical signal processing, sparse signal processing and their applications in radar, navigation and wireless communications.

He is currently on the editorial boards of IEEE TRANSACTIONS ON SIGNAL PROCESSING, *Digital Signal Processing*, and *IET Signal Processing*. He is also an elected member in Sensor Array and Multichannel (SAM) Technical Committee (TC) of the IEEE Signal Processing Society. In addition, he was elected an IET Fellow in 2018.

Jian-Kang Zhang (SM’09) received the B.S. degree in information science (mathematics) from Shaanxi Normal University, Xian, China, the M.S. degree in information and computational science (mathematics) from Northwest University, Xian, China, and the Ph.D. degree in electrical engineering from Xidian University, Xian, China, in 1983, 1988, and 1999, respectively.

He is currently an Associate Professor with the Department of Electrical and Computer Engineering, McMaster University, Hamilton, ON, Canada. He has hold research positions in McMaster University and Harvard University. His research interests include signal processing, digital communications, and signal detection and estimation. He is the coauthor of the paper that received the IEEE Signal Processing Society Best Young Author Award in 2008. He has served as an Associate Editor for the IEEE SIGNAL PROCESSING LETTERS and IEEE TRANSACTIONS ON SIGNAL PROCESSING. He is currently an Associate Editor for the *Journal of Electrical and Computer Engineering*.

Junhao Xie (M’02–SM’14) received the B.S. degree in electronic engineering from the Harbin Institute of Shipbuilding Engineering, Harbin, China, the M.S. degree in signal and information processing from the Harbin Engineering University, Harbin, China, and the Ph.D. degree in communication and information system from the Harbin Institute of Technology, Harbin, China, in 1992, 1995, and 2001 respectively.

From 2004 to 2006, he was a Visiting Scholar with the Curtin University of Technology, Perth, WA, Australia, where he dealt with radar remote sensing signal processing. He is currently a Professor with the Department of Electronic Engineering, Harbin Institute of Technology. His past and present research interests involve radar system analysis and modeling, array signal processing, target detection and estimation, and ocean remote sensing for shipborne high-frequency surface wave radar and inverse synthetic aperture radar.

Hing Cheung So (S’90–M’95–SM’07–F’15) was born in Hong Kong. He received the B.Eng. degree from the City University of Hong Kong, Hong Kong, and the Ph.D. degree from The Chinese University of Hong Kong, Hong Kong, in 1990 and 1995, respectively, both in electronic engineering. From 1990 to 1991, he was an Electronic Engineer with the Research and Development Division, Everex Systems Engineering, Ltd., Hong Kong. During 1995–1996, he was a Postdoctoral Fellow with The Chinese University of Hong Kong. From 1996 to 1999, he was a Research Assistant Professor with the Department of Electronic Engineering, City University of Hong Kong, where he is currently a Professor. His research interests include detection and estimation, fast and adaptive algorithms, multidimensional harmonic retrieval, robust signal processing, source localization, and sparse approximation.

He has been on the editorial boards of IEEE SIGNAL PROCESSING MAGAZINE (2014–2017), IEEE TRANSACTIONS ON SIGNAL PROCESSING (2010–2014), *Signal Processing* (2010–till present), and *Digital Signal Processing* (2011–till present). He was also a Lead Guest Editor for the IEEE JOURNAL OF SELECTED TOPICS IN SIGNAL PROCESSING, special issue on Advances in Time/Frequency Modulated Array Signal Processing in 2017. In addition, he was an elected member in Signal Processing Theory and Methods Technical Committee (2011–2016) of the IEEE Signal Processing Society where he was chair in the awards subcommittee (2015–2016).